

Koopman-based lifting techniques for nonlinear systems identification

A. Mauroy¹ and J. Goncalves²

¹ Department of Mathematics and Namur Center for Complex Systems (naXys), University of Namur, Belgium (email: alexandre.mauroy@unamur.be)

² Luxembourg Centre for Systems Biomedicine, University of Luxembourg, Belvaux, Luxembourg

Abstract

We develop a novel lifting technique for nonlinear system identification based on the framework of the Koopman operator. The key idea is to identify the linear (infinite-dimensional) Koopman operator in the lifted space of observables, instead of identifying the nonlinear system in the state space, a process which results in a linear method for nonlinear systems identification. The proposed lifting technique is an indirect method that does not require to compute time derivatives and is therefore well-suited to low-sampling rate datasets.

Considering different finite-dimensional subspaces to approximate and identify the Koopman operator, we propose two numerical schemes: the main method and the dual method. The main method is a parametric identification technique that can accurately reconstruct the vector field of a broad class of systems (including unstable, chaotic, and system with inputs). The dual method provides estimates of the vector field at the data points and is well-suited to identify high-dimensional systems with small datasets. The present paper describes the two methods, provide theoretical convergence results, and illustrate the lifting techniques with several examples.

1 Introduction

The problem of identifying the equations of a continuous-time dynamical system from time-series data has attracted considerable interest in many fields such as biology, finance, and engineering. It is also closely related to network inference, which aims at reconstructing the interactions between the different states of a system, a problem of paramount importance in systems biology. In many cases, the identification problem is more challenging due to the nonlinear nature of the systems and must be tackled with black-box methods (e.g. Wiener and Volterra series models [35], nonlinear auto-regressive models [15], neural network models [23], see also [30, 7] for a survey). In line with the classic approach to system identification, these methods typically deal with (long, highly-sampled) time-series and provide a relationship between the system inputs and outputs.

Partly motivated by the network identification problem, recent approaches have been developed in a context different from classic system identification, in order to identify the state dynamics of autonomous systems from observed states (e.g. Bayesian approach [25], SINDy algorithm [3]). These methods are *direct* methods which can be seen as static linear regression techniques seeking the best linear combination of known state time derivatives over a set of library functions (similar to the basis functions used in black-box models). However, they assume that the state time derivatives can be accurately estimated, a requirement that

becomes prohibitive if the sampling time is too low, the measurements too noisy, or the time-series too short. In these cases, there is a need for *indirect* methods that do not rely on a direct estimation of time derivatives. If we draw a parallel with linear systems, (linear) indirect methods identify the exponential matrix e^{AT_s} from snapshot data (with sampling time T_s) instead of the matrix A from approximative time derivatives (see [39]). The goal of this paper is to fill the gap by proposing an *indirect* method for nonlinear systems identification.

The approach proposed in this paper is based on the framework of the so-called Koopman operator [4, 10]. The Koopman operator is a linear infinite-dimensional operator that describes the evolution of observable-functions along the trajectories of the system. Starting with the seminal work of [21], several studies have investigated the interplay between the spectral properties of the operator and the properties of the associated system. This body of work yielded new methods for the analysis of nonlinear systems (e.g. global stability analysis [19], global linearization [13], monotone systems [20], delayed systems [22]). While the above-mentioned studies focus on systems described by a known vector field, the Koopman operator approach is also conducive to data analysis and directly connected to numerical schemes such as Dynamic Mode Decomposition (DMD) [1, 28, 29, 34]. This led to another set of techniques for data-driven analysis and control of nonlinear systems (observer synthesis [31], model predictive control [11], optimal control [8], power systems stability analysis [32], to list a few). In this context, this paper aims at connecting data to vector field, thereby bridging these two sets of methods.

The Koopman operator provides a linear representation of the nonlinear system in a lifted (infinite-dimensional) space of observable-functions. Our key idea is to exploit this lifting approach and *identify the linear Koopman operator in the space of observables*, instead of identifying the nonlinear system in the state space. Our numerical scheme proceeds in three steps: (1) lifting of the data, (2) identification of the Koopman operator, and (3) identification of the vector field. In the first step, snapshot data are lifted to the space of observables. In the second step, we derive two distinct methods. The main method consists in identifying a representation of the Koopman operator in a basis of functions (e.g. monomials). In contrast, a dual method is related to the representation of the operator in the “sample space”. The first two steps are directly related to a component of the Extended Dynamic Mode Decomposition (EDMD) [36] (main method) or inspired from kernel-based EDMD [37] (dual method). In the third step, we connect the vector field to the infinitesimal generator of the identified operator and solve a linear least squares problem to compute the linear combination of the vector field in a basis of library functions. As a by product, an intermediate step of the dual method also provides the values of the vector field at the sample points.

The proposed lifting technique has several advantages. First of all, it relies only on linear methods which are easy and efficient to implement. It is also well-suited to data acquired from short time-series with low sampling rates (e.g. data pairs generated from multiple trajectories). Although initially limited to polynomial vector fields, the main method works efficiently with a broad class of behaviors, including unstable and chaotic systems. In addition, the dual method is well-suited to identify large-dimensional systems and to reconstruct network topologies, in particular when the number of sample points is smaller than the unknown system parameters. Finally, lifting techniques can be extended to identify non-polynomial vector fields and open systems (with input or process noise).

The rest of the paper is organized as follows. In Section 2, we present the problem and introduce the general lifting technique used for system identification. Section 3 describes the main method and provides theoretical convergence results, while Section 4 discusses some

extensions of the methods to non-polynomial vector fields and open systems. In Section 5, we propose the dual method to identify high-dimensional systems with small datasets. The two methods are illustrated with several examples in Section 6, where the network reconstruction problem is also considered. Concluding remarks and perspectives are given in Section 7.

This paper builds on preliminary results presented in [18]. New contributions are the theoretical proofs of convergence (Sections 3.3 and 5.3), the extension to non-polynomial vector fields (Section 4.3), the dual method (Section 5), and the examples (Section 6).

2 Identification in the Koopman operator framework

2.1 Problem statement

We address the problem of identifying the vector field of a nonlinear system from time series generated by its dynamics. We consider the system

$$\dot{\mathbf{x}} = \mathbf{F}(\mathbf{x}), \quad \mathbf{x} \in \mathbb{R}^n \quad (1)$$

where the vector field $\mathbf{F}(\mathbf{x})$ is of the form

$$\mathbf{F}(\mathbf{x}) = \sum_{k=1}^{N_F} \mathbf{w}_k h_k(x). \quad (2)$$

The vectors $\mathbf{w}_k = (w_k^1 \cdots w_k^n)^T \in \mathbb{R}^n$ are unknown coefficients (to be identified) and the library functions h_k are assumed to be known. Note that some coefficients might be equal zero. Unless stated otherwise, we will consider that the vector field is polynomial, so that h_k are monomials: $h_k = p_k$ with

$$p_k(\mathbf{x}) \in \{x_1^{s_1} \cdots x_n^{s_n} \mid (s_1, \dots, s_n) \in \mathbb{N}^n, s_1 + \cdots + s_n \leq m_F\} \quad (3)$$

where m_F is the total degree of the polynomial vector field. The number of monomials in the sum (2) is given by $N_F = (m_F + n)! / (m_F! n!)$. For practical purposes, the sequence of monomials should be characterized by some order (e.g. lexicographic order, weight order). As shown in Section 4.3, the proposed method can also be generalized to other types of vector fields.

Our goal is to identify the vector field \mathbf{F} (i.e. the N_F coefficients \mathbf{w}_k) from K snapshot pairs $(\mathbf{x}_k, \mathbf{y}_k) \in X \times X$ of the system trajectories, where $X \subset \mathbb{R}^n$ is a compact set. We consider that these data points are obtained from noisy measurements, i.e.

$$\mathbf{y}_k = \varphi^{T_s}(\mathbf{x}_k(\mathbf{1} + \mathbf{v}_k)) \quad (4)$$

where $t \mapsto \varphi^t(\mathbf{x}_0)$ is a solution to (1) associated with the initial condition \mathbf{x}_0 and \mathbf{v}_k is a Gaussian random variable with zero mean and standard deviation σ_{meas} . Note that measurement noise is proportional to the state value. We assume that all pairs $(\mathbf{x}_k, \mathbf{y}_k)$ are obtained with the same sampling period T_s . However, they can belong to a unique time series or to different trajectories. Stochastic systems with process noise and systems with inputs will also be considered (see Section 4).

Remark 1. For numerical reasons, we will assume in general that the data points lie in a set $X \subset [-1, 1]^n$. If original data do not satisfy this assumption, then they can be rescaled to yield new data pairs $(\mathbf{x}'_k, \mathbf{y}'_k) = (\mathbf{x}_k/\alpha, \mathbf{y}_k/\alpha) \in [-1, 1]^{2n}$. These new pairs enable to identify a vector field $\mathbf{F}'(\mathbf{x})$ with coefficients $\mathbf{w}'_k = \alpha^{m_k-1} \mathbf{w}_k$, where m_k is the total degree of the monomial p_k . \diamond

2.2 Koopman operator

System (1) represents the state dynamics in \mathbb{R}^n . Alternatively, the system can be described in a lifted space \mathcal{F} of observable-functions $f : \mathbb{R}^n \rightarrow \mathbb{R}$. Provided that the observable functions are continuously differentiable, their dynamics in the lifted space are given by

$$\dot{f} = (\mathbf{F} \cdot \nabla)f, \quad f \in \mathcal{F}, \quad (5)$$

where \dot{f} denotes $\partial(f \circ \varphi^t)/\partial t$ (with a slight abuse of notation) and ∇ denotes the gradient (see e.g. [14]). In contrast to (1), the dynamics (5) are infinite-dimensional but linear.

While the flow induced by (1) in the state space is given by the nonlinear flow map φ , the flow induced by (5) in the lifted space is given by the linear semigroup of Koopman operators $U^t : \mathcal{F} \rightarrow \mathcal{F}$, $t \geq 0$. This semigroup governs the evolution of the observables along the trajectories, i.e.

$$U^t f = f \circ \varphi^t.$$

Under appropriate conditions (see Section 3.3), the semigroup of Koopman operators is strongly continuous and generated by the operator

$$L = \mathbf{F} \cdot \nabla \quad (6)$$

appearing in (5). In this case, we use the notation

$$U^t = e^{Lt}. \quad (7)$$

The operator L is called the infinitesimal generator of the Koopman operator and we denote its domain by $\mathcal{D}(L)$.

2.3 Linear identification in the lifted space

There is a one-to-one correspondence between systems of the form (1) and lifted systems (5), or equivalently between the flow φ^t and the semigroup of Koopman operators U^t . Exploiting this equivalence, we propose to solve the identification problem in the lifted space instead of the state space. This can be done in three steps (see Figure 1).

1. **Lifting of the data.** Snapshots pairs $(\mathbf{x}_k, \mathbf{y}_k)$ are lifted to the space of observable by constructing new pairs of the form $(g(\mathbf{x}_k), g(\mathbf{y}_k))$ for some $g \in \mathcal{F}$. The functions g are assumed to be continuously differentiable and we call them *basis functions*. It follows from (4) that

$$g(\mathbf{y}_k) = g(\varphi^{T_s}(\mathbf{x}_k(\mathbf{1} + \mathbf{v}_k))) = U^{T_s}g(\mathbf{x}_k) + e_k \quad (8)$$

where $e_k \approx \nabla g(\varphi^{T_s}(\mathbf{x}_k)) \cdot \mathbf{v}_k \varphi^{T_s}(\mathbf{x}_k) + \mathcal{O}(\|\mathbf{v}_k \varphi^{T_s}(\mathbf{x}_k)\|^2)$ is a (small) error due to the measurement noise.

2. **Identification of the Koopman operator.** A finite-dimensional projection of the Koopman operator is obtained through a classic linear identification method that is similar to a component of the Extended Dynamic Mode Decomposition (EDMD) algorithm [36]. It follows from (7) that this yields (an approximation of) the infinitesimal generator L of the Koopman operator.
3. **Identification of the vector field.** Using (6), we can finally obtain the vector field \mathbf{F} .

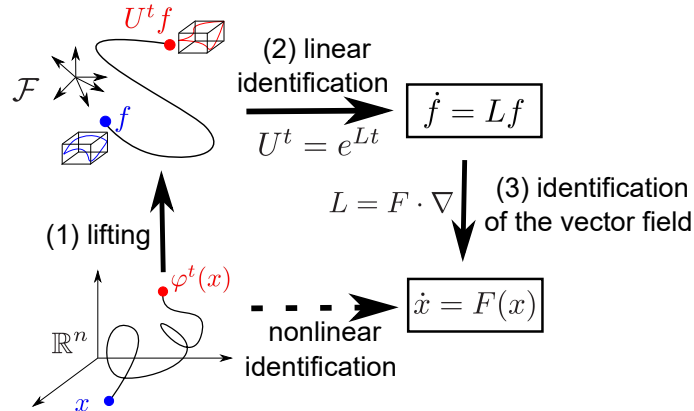


Figure 1: Classical nonlinear system identification is performed directly in the state space. In contrast, the proposed lifting technique consists of three steps: (1) lifting of the data; (2) linear identification of the Koopman operator in the lifted space; (3) identification of the vector field.

3 The main lifting method

3.1 Description of the method

This section describes in detail the three steps of our main method. The first step and the first part of the second step are related to a component of the EDMD algorithm (see [36] for more details).

3.1.1 First step: Lifting of the data

The data must be lifted to the infinite-dimensional space \mathcal{F} of observables. However, the method has to be numerically tractable and is developed in a finite-dimensional linear subspace $\mathcal{F}_N \subset \mathcal{F}$ spanned by a basis of N linearly independent functions. The choice of basis functions $\{g_k\}_{k=1}^N$ can be arbitrary (e.g. Fourier basis, radial basis functions), but might affect the method performances. At least the functions should form a proper complete basis in the space $L_2(X)$ (see Section 3.3). Since the vector field is assumed to be polynomial, we naturally choose the basis of monomials $\{g_k\}_{k=1}^N = \{p_k\}_{k=1}^N$ with total degree less or equal to m to facilitate the representation of the Koopman operator. The number of basis functions is equal to $N = (n + m)! / (n! m!)$.

For each snapshot pair $(\mathbf{x}_k, \mathbf{y}_k) \in \mathbb{R}^{n \times 2}$, $k \in \{1, \dots, K\}$, we construct a new pair $(\mathbf{p}(\mathbf{x}_k), \mathbf{p}(\mathbf{y}_k)) \in \mathbb{R}^{N \times 2}$, where $\mathbf{p}(\mathbf{x}) = (p_1(\mathbf{x}), \dots, p_N(\mathbf{x}))^T$ denotes the vector of basis monomials. In the following, we will also use the $K \times N$ matrices

$$\mathbf{P}_x = \begin{pmatrix} \mathbf{p}(\mathbf{x}_1)^T \\ \vdots \\ \mathbf{p}(\mathbf{x}_K)^T \end{pmatrix} \quad \mathbf{P}_y = \begin{pmatrix} \mathbf{p}(\mathbf{y}_1)^T \\ \vdots \\ \mathbf{p}(\mathbf{y}_K)^T \end{pmatrix}. \quad (9)$$

3.1.2 Second step: Identification of the Koopman operator

Now we proceed to the identification of the Koopman operator U^t , for $t = T_s$. More precisely, we will identify the finite-rank operator $U_N^t : \mathcal{F}_N \rightarrow \mathcal{F}_N$ of the form $U_N^t = P_N U^t|_{\mathcal{F}_N}$, where

$P_N : \mathcal{F} \rightarrow \mathcal{F}_N$ is a projection operator onto the subspace \mathcal{F}_N and $U^t|_{\mathcal{F}_N} : \mathcal{F}_N \rightarrow \mathcal{F}$ is the restriction of the Koopman operator to \mathcal{F}_N . Considering

$$f = \mathbf{a}^T \mathbf{p}, \quad U_N^{T_s} f = \mathbf{b}^T \mathbf{p}, \quad (10)$$

we can define a matrix $\bar{\mathbf{U}}_N \in \mathbb{R}^{N \times N}$ such that

$$\bar{\mathbf{U}}_N \mathbf{a} = \mathbf{b}. \quad (11)$$

The matrix $\bar{\mathbf{U}}_N$ is a representation of the projected Koopman operator $U_N^{T_s}$. It also provides an approximate finite-dimensional linear description of the nonlinear system. This description is not obtained through local linearization techniques and is valid globally.

It follows from (10) and (11) that

$$U_N^{T_s} f = U_N^{T_s} (\mathbf{a}^T \mathbf{p}) = (\bar{\mathbf{U}}_N \mathbf{a})^T \mathbf{p} \quad (12)$$

and, since (12) holds for all \mathbf{a} , we have

$$U_N^{T_s} \mathbf{p}^T = \mathbf{p}^T \bar{\mathbf{U}}_N, \quad (13)$$

where the operator $U_N^{T_s}$ acts on each component of the vector \mathbf{p} . By considering each column separately, we obtain $P_N U^{T_s} p_j = U_N^{T_s} p_j = \mathbf{c}_j^T \mathbf{p}$, where \mathbf{c}_j is the j th column of $\bar{\mathbf{U}}_N$. This shows that each column of $\bar{\mathbf{U}}_N$ is related to the projection onto \mathcal{F}_N of the image of a basis function p_j through the Koopman operator U^{T_s} .

There are an infinity of possible projections P_N . We consider here a discrete orthogonal projection yielding the least squares fit at the points \mathbf{x}_k , $k = 1, \dots, K$, with $K \geq N$:

$$P_N g = \underset{\tilde{g} \in \text{span}\{p_1, \dots, p_N\}}{\text{argmin}} \sum_{k=1}^K |\tilde{g}(\mathbf{x}_k) - g(\mathbf{x}_k)|^2. \quad (14)$$

This corresponds to the least squares solution

$$P_N g = \mathbf{p}^T \mathbf{P}_x^\dagger \begin{pmatrix} g(\mathbf{x}_1) \\ \vdots \\ g(\mathbf{x}_K) \end{pmatrix}$$

where \mathbf{P}^\dagger denotes the pseudoinverse of \mathbf{P} . For $g = U^{T_s} p_j$, we obtain

$$P_N(U^{T_s} p_j) = \mathbf{p}^T \mathbf{P}_x^\dagger \begin{pmatrix} U^{T_s} p_j(\mathbf{x}_1) \\ \vdots \\ U^{T_s} p_j(\mathbf{x}_K) \end{pmatrix} \approx \mathbf{p}^T \mathbf{P}_x^\dagger \begin{pmatrix} p_j(\mathbf{y}_1) \\ \vdots \\ p_j(\mathbf{y}_K) \end{pmatrix}$$

where we used (8) evaluated at the states \mathbf{x}_k and assumed that the error e_k due to measurement noise is small. Equivalently, we have

$$U_N^{T_s} \mathbf{p}^T \approx \mathbf{p}^T \mathbf{P}_x^\dagger \mathbf{P}_y$$

so that (13) yields

$$\bar{\mathbf{U}}_N \approx \mathbf{P}_x^\dagger \mathbf{P}_y. \quad (15)$$

Inspired by (7), we finally compute

$$\bar{\mathbf{L}}_{\text{data}} = \frac{1}{T_s} \log(\mathbf{P}_x^\dagger \mathbf{P}_y), \quad (16)$$

where the function \log denotes the (principal) matrix logarithm. The matrix $\bar{\mathbf{L}}_{\text{data}}$ is an approximation of the matrix representation $\bar{\mathbf{L}}_N$ of $L_N = P_N L|_{\mathcal{F}_N}$, where $L_N f = \mathbf{p}^T (\bar{\mathbf{L}}_N \mathbf{a})$ for all $f = \mathbf{p}^T \mathbf{a}$. A rigorous justification is given in Section 3.3.

Remark 2. Even with no measure noise, $\bar{\mathbf{L}}_{\text{data}}$ is only an approximation of $\bar{\mathbf{L}}_N$. Indeed, $\bar{\mathbf{L}}_{\text{data}}$ is the matrix representation of the finite-rank operator $\frac{1}{T_s} \log(P_N U^{T_s}|_{\mathcal{F}_N}) = \frac{1}{T_s} \log(P_N e^{L T_s}|_{\mathcal{F}_N}) \neq P_N L|_{\mathcal{F}_N}$. The two matrices $\bar{\mathbf{L}}_{\text{data}}$ and $\bar{\mathbf{L}}_N$ are identical only in the limit $N \rightarrow \infty$ and under some additional conditions related to the non-uniqueness of the matrix logarithm (see Section 3.3). \diamond

3.1.3 Third step: Identification of the vector field

We are now in position to identify the coefficients $\mathbf{w}_k = (w_k^1 \cdots w_k^n)$ of the vector field. To do so, we express a matrix representation of L in terms of the coefficients w_k^j . Then, we can find the coefficients by comparing the matrix representation with the matrix $\bar{\mathbf{L}}_{\text{data}}$ obtained from data.

Computation of a matrix representation of L . It follows from (2) and (6) that

$$L = \sum_{j=1}^n \sum_{k=1}^{N_F} w_k^j L_k^j \quad (17)$$

with the linear operators

$$L_k^j = p_k \frac{\partial}{\partial x_j}, \quad j = 1, \dots, n, \quad k = 1, \dots, N_F. \quad (18)$$

Recalling that the vector field is a polynomial of total degree less or equal to m_F , we clearly see that the operators L_k^j map polynomials of total degree less or equal to m_0 to polynomials of total degree less or equal to $m = m_0 + m_F - 1$. It follows that the operator $L_k^j|_{\mathcal{F}_{N_0}} : \mathcal{F}_{N_0} \rightarrow \mathcal{F}_N$ is finite-rank (note that $P_N L_k^j|_{\mathcal{F}_{N_0}} = L_k^j|_{\mathcal{F}_{N_0}}$) and has a matrix representation $\bar{\mathbf{L}}_k^j \in \mathbb{R}^{N \times N_0}$, with $N_0 = (m_0 + n)! / (m_0! n!) \leq N = (m + n)! / (m! n!)$. Denoting by \mathbf{p}^{m_0} and \mathbf{p}^m the vectors of monomials of total degree less or equal to m_0 and m , respectively, we have

$$L_k^j f = (\bar{\mathbf{L}}_k^j \mathbf{a})^T \mathbf{p}^m \quad \forall f = \mathbf{a}^T \mathbf{p}^{m_0}.$$

It follows that $L_k^j \mathbf{p}^{m_0} = (\bar{\mathbf{L}}_k^j)^T \mathbf{p}^m$, which implies that the l th column of $\bar{\mathbf{L}}_k^j$ corresponds to the expansion of $L_k^j p_l$ in the basis of monomials \mathbf{p}^m .

Next, we define an index function $\Psi(k) = (\psi_1(k), \dots, \psi_n(k))$ that encodes the order of the monomials in the vector \mathbf{p} , i.e. $p_k(\mathbf{x}) = x_1^{\psi_1(k)} \cdots x_n^{\psi_n(k)}$. Then (18) implies that

$$L_k^j p_l = \psi_j(l) p_{\Psi^{-1}(\Psi(k) + \Psi(l) - \mathbf{e}_j)}$$

where $\mathbf{e}_j \in \mathbb{R}^n$ is the j th unit vector and the entries of $\bar{\mathbf{L}}_k^j$ are given by

$$\left[\bar{\mathbf{L}}_k^j\right]_{il} = \begin{cases} \psi_j(l) & \text{if } \Psi(i) = \Psi(k) + \Psi(l) - \mathbf{e}_j, \\ 0 & \text{otherwise.} \end{cases} \quad (19)$$

Note that the matrices $\bar{\mathbf{L}}_k^j$ can also be obtained by multiplying a multiplication matrix and a differentiation matrix (see [19] for more details). Finally, it follows from (17) that the matrix representation of $P_N L|_{\mathcal{F}_{N_0}} = L|_{\mathcal{F}_{N_0}}$ is given by

$$\bar{\mathbf{L}} = \sum_{j=1}^n \sum_{k=1}^{N_F} w_k^j \bar{\mathbf{L}}_k^j. \quad (20)$$

Computation of the coefficients w_k^n . In the previous section, we have derived a matrix representation $\bar{\mathbf{L}}$ of $P_N L|_{\mathcal{F}_{N_0}}$. An approximation of this matrix representation is also given by the $N \times N_0$ matrix $\left[\bar{\mathbf{L}}_{\text{data}}\right]_{N_0}$, constructed with the N_0 columns of (16) associated with monomials of total degree less or equal to m_0 . Note that by disregarding the $N - N_0$ remaining columns in (16), we only consider monomials that are mapped by L onto the span of basis monomials of total degree less or equal to m , for which the finite Galerkin projection —i.e. the identity in this case— is exact (see also the discussion in Section 4.3). Then, it follows from (20) that the equality

$$\left[\bar{\mathbf{L}}_{\text{data}}\right]_{N_0} \approx \sum_{j=1}^n \sum_{k=1}^{N_F} w_k^j \bar{\mathbf{L}}_k^j \quad (21)$$

yields a linear set of equations, whose solutions \hat{w}_k^j are the estimates of the nN_F coefficients w_k^j . If $m = 1$, we have $N_0 = n + 1$ and $N = N_F$. Moreover, $\Psi_j(l) = 1$ if $\Psi(l) = \mathbf{e}_j$ and $\Psi_j(l) = 0$ otherwise. Using (19) and (21), we obtain in this case

$$\hat{w}_k^j = \left[\bar{\mathbf{L}}_{\text{data}}\right]_{kl}$$

with l such that $\Psi(l) = \mathbf{e}_j$. Indeed, since $L_N f = \mathbf{p}^T (\bar{\mathbf{L}}_N \mathbf{a})$ for all $f = \mathbf{p}^T \mathbf{a}$, it follows that

$$P_N (\mathbf{F} \cdot \nabla p_l) = \mathbf{p}^T \bar{\mathbf{L}}_N \mathbf{e}_l. \quad (22)$$

Since $\Psi(l) = \mathbf{e}_j$ (i.e. p_l is a monomial of degree 1), we also have

$$P_N (\mathbf{F} \cdot \nabla p_l) = P_N F_j = F_j, \quad (23)$$

so that $F_j = \mathbf{p}^T (\bar{\mathbf{L}}_N \mathbf{e}_l) \approx \mathbf{p}^T (\bar{\mathbf{L}}_{\text{data}} \mathbf{e}_l)$, i.e. the l th column of $\bar{\mathbf{L}}_{\text{data}}$ contains the estimates \hat{w}_k^j .

If $m > 1$, the number of equations is greater than nN_F and the set of equations is overdetermined. The estimates \hat{w}_k^j are obtained in this case by the least squares solution to the system

$$\begin{pmatrix} \hat{\mathbf{w}}_1 \\ \vdots \\ \hat{\mathbf{w}}_{N_F} \end{pmatrix} = \begin{pmatrix} \left| \text{vec}(\bar{\mathbf{L}}_1^1) \right. & \cdots & \left| \text{vec}(\bar{\mathbf{L}}_1^n) \right. & \cdots & \left| \text{vec}(\bar{\mathbf{L}}_{N_F}^1) \right. & \cdots & \left| \text{vec}(\bar{\mathbf{L}}_{N_F}^n) \right. \\ \vdots & & \vdots & & \vdots & & \vdots \end{pmatrix}^\dagger \text{vec} \left(\left[\bar{\mathbf{L}}_{\text{data}}\right]_{N_0} \right) \quad (24)$$

where \mathbf{vec} stands for the vectorization of the matrix. Some entries of $\bar{\mathbf{L}}_k^j$ are zero for all j and k , so that the corresponding entries of $\bar{\mathbf{L}}$ do not depend on the values \hat{w}_k^j and the related equalities in (24) can be disregarded.

Remark 3 (Nonlinear least squares problem). The identification problem could also be performed at the level of the Koopman semigroup. However solving the equality $\bar{\mathbf{U}} = e^{\bar{\mathbf{L}}T_s}$ (with a square matrix $\bar{\mathbf{L}}$) amounts to solving a (nonconvex) nonlinear least squares problem. This might also be equivalent to solving the direct identification problem with an exact Taylor discretization of time-derivatives [9]. Numerical simulations suggest that better results are obtained by solving (21). \diamond

Remark 4 (Estimation of the vector field). If needed, the method can directly provide the values $\mathbf{F}(\mathbf{x}_k)$ of the vector field. Evaluating (22) and (23) at \mathbf{x}_k for all $k = 1, \dots, K$ and considering $\bar{\mathbf{L}}_N \approx \bar{\mathbf{L}}_{\text{data}}$, we obtain an approximation \hat{F}_j of the vector field given by

$$\begin{pmatrix} \hat{F}_j(\mathbf{x}_1) \\ \vdots \\ \hat{F}_j(\mathbf{x}_K) \end{pmatrix} = \mathbf{P}_x (\bar{\mathbf{L}}_{\text{data}} \mathbf{e}_l) \quad (25)$$

with $\Psi(l) = \mathbf{e}_j$. This is quite similar to the approach developed with the dual method presented in Section 5. \diamond

3.2 Algorithm

Our main lifting method for system identification is summarized in the following algorithm.

Algorithm 1 Main lifting method for nonlinear system identification

- Input:** Snapshot pairs $\{(\mathbf{x}_k, \mathbf{y}_k)\}_{k=1}^K$, $\mathbf{x}_k \in \mathbb{R}^n$; sampling period T_s ; integers $m_0 \geq 1$ and $m_F \geq 0$.
Output: Estimates \hat{w}_k^j .
- 1: $m := m_0 + m_F - 1$;
 - 2: $N_0 := (m_0 + n)! / (m_0! n!)$; $N := (m + n)! / (m! n!)$; $N_F := (m_F + n)! / (m_F! n!)$
 - 3: **if** $N > K$ **then**
 - 4: Increase K (add snapshot pairs) or decrease m_0 or m
 - 5: **end if**
 - 6: Construct the $K \times N$ matrices \mathbf{P}_x and \mathbf{P}_y defined in (9)
 - 7: Compute the $N \times N$ matrix $\bar{\mathbf{L}}_{\text{data}}$ defined in (16)
 - 8: **if** $m_0 = 1$ **then**
 - 9: $\hat{w}_k^j := [\bar{\mathbf{L}}_{\text{data}}]_{kl}$, with l such that $\Psi_l = \mathbf{e}_j$
 - 10: **else**
 - 11: Construct the $N \times N_0$ matrices $\bar{\mathbf{L}}_k^j$ using (19)
 - 12: \hat{w}_k^j are given by (24)
 - 13: **end if**
-

3.3 Theoretical results

In this section, we prove the convergence of Algorithm 1 in optimal conditions, i.e. with an infinite number of data points and basis functions, and an arbitrarily high sampling rate.

We consider the space $\mathcal{F} = L^2(X)$ (where $\|\cdot\|$ is the L^2 norm) and the subspace \mathcal{F}_N spanned by the monomials $\{p_k\}_{k=1}^N$. The projection operator $P_N : L^2(X) \rightarrow \mathcal{F}_N$ is the discrete L^2 projection. We first have the following lemma.

Lemma 1. *Assume that the flow induced by (1) is invertible and nonsingular¹, and that X is forward-invariant (i.e. $\varphi^t(X) \subseteq X$ for all $t > 0$) or backward-invariant² (i.e. $\varphi^{-t}(X) \subseteq X$ for all $t > 0$). If*

$$\|P_N f - f\| \rightarrow 0 \tag{26}$$

for all $f \in L^2(X)$ as $N \rightarrow \infty$, then the semigroup of Koopman operators $U^t : L^2(X) \rightarrow L^2(X)$ and the infinitesimal generator $L : \mathcal{D}(L) \rightarrow L^2(X)$ satisfy

$$\|(P_N U^t - e^{P_N L t}) f\| \rightarrow 0$$

for all $f \in L^2(X)$ as $N \rightarrow \infty$.

Proof. We first check that the semigroup U^t is strongly continuous. For continuous functions $g : X \rightarrow \mathbb{R}$, which are dense in $L^2(X)$, we have

$$\lim_{t \rightarrow 0} \|g - U^t g\| = 0.$$

Moreover, we have

$$\|U^t f\|^2 = \int_X |U^t f(x)|^2 dx = \int_{\varphi^t(X)} |f(x)|^2 |J_{\varphi^{-t}}(x)| dx \leq \max_{x \in X} |J_{\varphi^{-t}}(x)| \|f\|^2$$

or equivalently

$$\frac{\|U^t f\|^2}{\|f\|^2} \leq \max_{x \in X} |J_{\varphi^t}(x)|^{-1}$$

where $|J_{\varphi^t}(x)|$ is the determinant of the Jacobian matrix of $\varphi^t(x)$. Since the flow is nonsingular, $|J_{\varphi^t}(x)| \neq 0$ implies that U^t is bounded. It follows that the semigroup of Koopman operators U^t is strongly continuous (see e.g. [5, Proposition I.5.3(c)]).

Next, (26) implies that $\|P_N L f - L f\| \rightarrow 0$ for all $f \in \mathcal{D}(L)$ as $N \rightarrow \infty$. Then, it follows from the Trotter-Kato approximation theorem (see e.g. [5, Theorem 4.8]) that

$$\|e^{P_N L t} f - U^t f\| \rightarrow 0$$

for all $f \in L^2(X)$ as $N \rightarrow \infty$. Finally, using again (26), we obtain

$$\|e^{P_N L t} f - P_N U^t f\| \leq \|e^{P_N L t} f - U^t f\| + \|U^t f - P_N U^t f\| \rightarrow 0$$

for all $f \in L^2(X)$ as $N \rightarrow \infty$. □

We are now in position to show that Algorithm 1 yields exact estimates \hat{w}_k^j of the vector field coefficients in optimal conditions.

¹The flow is nonsingular if $\mu(A) \neq 0$ implies $\mu(\varphi^t(A)) \neq 0$ for all $A \in \mathbb{R}^n$ and all $t > 0$, where μ is the Lebesgue measure. This is a generic condition that is satisfied when the vector field F is Lipschitz continuous, for instance.

²When X is backward-invariant, we assume that $f(x) = 0$ for all $x \notin X$ and all $f \in \mathcal{F}$, so that U^t is a well-defined semigroup.

Theorem 1. Assume that the sample points $\mathbf{x}_k \in X$ are uniformly randomly distributed in a compact forward or backward invariant set $X \subset [-1, 1]^n$, and consider $\mathbf{y}_k = \varphi^{T_s}(\mathbf{x}_k)$ (no measurement noise) where φ^t is invertible and nonsingular. If the Algorithm 1 is used with the data pairs $\{\mathbf{x}_k, \mathbf{y}_k\}_{k=1}^K$, then $\hat{w}_k^j \rightarrow w_k^j$ for all $j = 1, \dots, n$ and $k = 1, \dots, N_F$ as $N \rightarrow \infty$, $K \rightarrow \infty$, and $T_s \rightarrow 0$.

Proof. Recall that $\bar{\mathbf{L}}_N$ and $\bar{\mathbf{L}}$ are the matrix representations of $L_N = P_N L|_{\mathcal{F}_N}$ and $P_N L|_{\mathcal{F}_{N_0}}$, respectively. Using (20), we have

$$\sum_{j=1}^n \sum_{k=1}^{N_F} (w_k^j - \hat{w}_k^j) \bar{\mathbf{L}}_k^j = \bar{\mathbf{L}} - \sum_{j=1}^n \sum_{k=1}^{N_F} \hat{w}_k^j \bar{\mathbf{L}}_k^j = \left(\bar{\mathbf{L}} - [\bar{\mathbf{L}}_{\text{data}}]_{N_0} \right) + \left([\bar{\mathbf{L}}_{\text{data}}]_{N_0} - \sum_{j=1}^n \sum_{k=1}^{N_F} \hat{w}_k^j \bar{\mathbf{L}}_k^j \right), \quad (27)$$

where $[\bar{\mathbf{L}}_{\text{data}}]_{N_0}$ is constructed with N_0 columns of $\bar{\mathbf{L}}_{\text{data}}$. We first show that

$$\bar{\mathbf{L}} - [\bar{\mathbf{L}}_{\text{data}}]_{N_0} \rightarrow \mathbf{0} \quad (28)$$

as $N \rightarrow \infty$. Since $\mathbf{x}_k \in X$, the discrete orthogonal projection (14) is a well-defined projection from $L^2(X)$ to the subspace $\mathcal{F}_N \subset L^2(X)$ spanned by the monomials $\{p_k\}_{k=1}^N$. In addition, as $K \rightarrow \infty$ (which is implied by $N \rightarrow \infty$), the projection P_N converges in the strong operator topology to the orthogonal L^2 projection (see e.g. [12] for a proof) and since the monomials form a complete basis of $L^2(X)$, it is clear that the orthogonal projection $P_N : \mathcal{F} \rightarrow \mathcal{F}$ converges in the strong operator topology to the identity operator as $N \rightarrow \infty$. This implies that (26) is satisfied. Supposing that

$$(P_N U^{T_s} - e^{P_N L T_s}) p_l = \mathbf{a}^T \mathbf{p}$$

with $\mathbf{a} \in \mathbb{R}^N$ and where $p_l \in \mathcal{F}_N$ is a monomial, we can apply Lemma 1 and obtain

$$\left\| (P_N U^{T_s} - e^{P_N L T_s}) p_l \right\| = \left\| \mathbf{a}^T \mathbf{p} \right\| \rightarrow 0$$

as $N \rightarrow \infty$. Since the monomials form a complete basis of linearly independent functions, we have that $\mathbf{a} \rightarrow \mathbf{0}$. It is clear that \mathbf{a} is the l th column of $\bar{\mathbf{U}}_N - e^{\bar{\mathbf{L}}_N T_s}$, so that $\bar{\mathbf{U}}_N - e^{\bar{\mathbf{L}}_N T_s} \rightarrow \mathbf{0}$, or equivalently $\frac{1}{T_s} \log \bar{\mathbf{U}}_N - \frac{1}{T_s} \log e^{\bar{\mathbf{L}}_N T_s} \rightarrow \mathbf{0}$ as $N \rightarrow \infty$. Since there is no measurement noise, (15) and (16) imply that $\frac{1}{T_s} \log \bar{\mathbf{U}}_N = \bar{\mathbf{L}}_{\text{data}}$. In addition, the spectrum of $\bar{\mathbf{L}}_N$ is a subset of $\mathbb{R} \times [-i\pi/T_s, i\pi/T_s] \rightarrow \mathbb{C}$ as $T_s \rightarrow 0$, so that $\frac{1}{T_s} \log e^{\bar{\mathbf{L}}_N T_s} = \bar{\mathbf{L}}_N$. Finally, this implies that $\bar{\mathbf{L}}_{\text{data}} - \bar{\mathbf{L}}_N \rightarrow 0$ and since $[\bar{\mathbf{L}}_N]_{N_0} = \bar{\mathbf{L}}$, we obtain (28).

Now, we show that

$$[\bar{\mathbf{L}}_{\text{data}}] - \sum_{j=1}^n \sum_{k=1}^{N_F} \hat{w}_k^j \bar{\mathbf{L}}_k^j \rightarrow \mathbf{0}. \quad (29)$$

If $m_0 = 1$ (i.e. $N_0 = n + 1$), the estimates \hat{w}_k^j are the exact solution to (21), so that (29) holds. If $m_0 > 1$, \hat{w}_k^j is the least squares solution to (21), so that

$$\begin{aligned} \left\| [\bar{\mathbf{L}}_{\text{data}}] - \sum_{j=1}^n \sum_{k=1}^{N_F} \hat{w}_k^j \bar{\mathbf{L}}_k^j \right\|_{\text{Fr}} &= \min_{w_k^j} \left\| [\bar{\mathbf{L}}_{\text{data}}] - \sum_{j=1}^n \sum_{k=1}^{N_F} w_k^j \bar{\mathbf{L}}_k^j \right\|_{\text{Fr}} \\ &\leq \left\| [\bar{\mathbf{L}}_{\text{data}}] - \bar{\mathbf{L}} \right\|_{\text{Fr}} + \min_{w_k^j} \left\| \bar{\mathbf{L}} - \sum_{j=1}^n \sum_{k=1}^{N_F} w_k^j \bar{\mathbf{L}}_k^j \right\|_{\text{Fr}} \rightarrow 0 \end{aligned}$$

where $\|\cdot\|_{\text{Fr}}$ denotes the Frobenius norm. Note that we used (28) and the minimum is attained with the exact coefficients w_k^j , which are the solution to (20). The above inequality implies (29). Then, (27), (28), and (29) yield

$$\sum_{j=1}^n \sum_{k=1}^{N_F} (w_k^j - \hat{w}_k^j) \bar{\mathbf{L}}_k^j \rightarrow \mathbf{0}.$$

Consider the set \mathcal{L} of indices l such that p_l is a monomial of degree 1, i.e. $\mathcal{L} = \{l : \Psi(l) = \mathbf{e}_{j'} \text{ for some } j'\}$. It follows from (19) that, for $l \in \mathcal{L}$,

$$\left[\bar{\mathbf{L}}_k^j \right]_{il} = \begin{cases} \delta_{jj'} & \text{if } \Psi(i) = \Psi(k) + \mathbf{e}_{j'} - \mathbf{e}_j \text{ and } \Psi(l) = \mathbf{e}_{j'}, \\ 0 & \text{otherwise,} \end{cases}$$

where $\delta_{jj'}$ denotes the Kronecker delta. Equivalently, for $l \in \mathcal{L}$, $\left[\bar{\mathbf{L}}_k^j \right]_{il} \neq 0$ if and only if $i = k$ and $\Psi(l) = \mathbf{e}_j$. This implies that each matrix $\bar{\mathbf{L}}_k^j$ has only one nonzero entry in its l th columns with $l \in \mathcal{L}$. In addition, this nonzero entry lies in a different pair of row and column for each matrix. It follows that the matrices $\bar{\mathbf{L}}_k^j$ are linearly independent, so that $w_k^j - \hat{w}_k^j \rightarrow 0$ for all $j = 1, \dots, n$ and $k = 1, \dots, N_F$, which concludes the proof. \square

Remark 5. The result of Theorem 1 could be extended to other basis functions h_k , but this is beyond the scope of this paper. The main requirement for this more general result to hold is that the functions $\{(L_k^j h_1, \dots, L_k^j h_{N_0})\}_{j,k}$ should be linearly independent in \mathcal{F}^{N_0} . \diamond

According to Theorem 1, Algorithm 1 identifies exactly the vector field, even if the data are collected in a small region of the state space. However, the result requires optimal conditions, i.e. an infinite number of data points ($K \rightarrow \infty$) and an infinite sampling frequency ($T_s \rightarrow 0$). The infinite number of data points is needed to represent the Koopman operator exactly with an infinite basis. Note that the requirement to collect the data points on an invariant set might not always be satisfied in practice. This is however a technical condition that ensures that U^t is a well-defined semigroup of operators on $[0, T_s]$, which is trivially satisfied in the limit $t = T_s \rightarrow 0$. The infinite sampling frequency ensures that the eigenvalues of $T_s \bar{\mathbf{L}}_N$ remain in the strip $\{z \in \mathbb{C} : |\Im\{z\}| < \pi\}$ as $N \rightarrow \infty$, so that $\log(\exp(T_s \bar{\mathbf{L}}_N)) = T_s \bar{\mathbf{L}}_N$. This issue is related to the so-called system aliasing and is discussed with more details in [39]. Intuitively, an infinite sampling rate is needed to capture the infinity of frequencies that characterizes a nonlinear system. In practice, for a finite value N , the eigenvalues of $\bar{\mathbf{L}}_N$ are bounded and correspond to the dominant frequencies of the dynamics. In this case, good results can be obtained with a finite—and possibly large—sampling period T_s , as shown with some examples in Section 6. The sampling period can even be arbitrarily large when all the eigenvalues of L are real.

The above theoretical results are valid only when there is no measurement noise. In presence of noise, there is no guarantee that the method will provide an exact estimation of the vector field coefficients w_k^j , even in the optimal conditions considered in Theorem 1. The estimator is actually biased and not consistent. This is due to the lifting of the data. Indeed, if the measurement noise \mathbf{v}_k has zero mean data points, then it is clear that the lifted data $p(\mathbf{x}_k(1 + \mathbf{v}_k))$ do not have zero mean, which introduces a bias in the solution to the least squares problem (15). The algorithm might be improved to tackle this issue, but we leave this for future research.

4 Extensions

We now consider several extensions of the proposed method, which allow to identify open systems driven by a known input or a white noise (i.e. process noise) and to identify systems with non-polynomial vector fields.

4.1 Systems with inputs

Consider an open dynamical system of the form

$$\dot{\mathbf{x}} = \mathbf{F}(\mathbf{x}, \mathbf{u}(t)) \quad (30)$$

with $\mathbf{x} \in \mathbb{R}^n$ and with the input $u \in \mathcal{U} : \mathbb{R}^+ \rightarrow \mathbb{R}^p$. We define the associated flow $\varphi : \mathbb{R}^+ \times \mathbb{R}^n \times \mathcal{U}$ so that $t \mapsto \varphi(t, \mathbf{x}, \mathbf{u}(\cdot))$ is a solution of (30) with the initial condition \mathbf{x} and the input $\mathbf{u}(\cdot)$. Following the generalization proposed in [2, 27], we consider observables $f : \mathbb{R}^n \times \mathbb{R}^p \rightarrow \mathbb{R}$ and define the semigroup of Koopman operators

$$U^t f(\mathbf{x}, \mathbf{u}) = f(\varphi^t(\mathbf{x}, \mathbf{u}(\cdot) = \mathbf{u}), \mathbf{u})$$

where $\mathbf{u}(\cdot) = \mathbf{u}$ is a constant input. In this case, \mathbf{u} can be considered as additional state variables and the above operator is the classic Koopman operator for the augmented system $\dot{\mathbf{x}} = \mathbf{F}(\mathbf{x}, \mathbf{u})$, $\dot{\mathbf{u}} = \mathbf{0}$. In particular, the infinitesimal generator is still given by (6).

It follows that the method proposed in Sections 3.1.1 and 3.1.2 can be used if

$$\varphi^{T_s}(\mathbf{x}, \mathbf{u}(\cdot)) \approx \varphi^{T_s}(\mathbf{x}, \mathbf{u}(\cdot) = \mathbf{u}(0)).$$

This condition holds when the input can be considered as constant between two snapshots (zero-order hold assumption), or equivalently if the sampling rate is high enough. The matrix $\bar{\mathbf{U}}_N$ is now obtained with snapshot pairs $([\mathbf{x}_k, \mathbf{u}_k], [\mathbf{y}_k, \mathbf{u}_k]) \in \mathbb{R}^{(n+p) \times 2}$ and the rest of the procedure follows on similar lines with the augmented state space \mathbb{R}^{n+p} . The efficiency of the identification method in the case of systems with inputs is shown in Section 6.2.

4.2 Process noise

We have considered so far only measurement noise. We show that the proposed method is also robust to process noise. Consider a system described by the stochastic differential equation

$$\dot{x}_k = F_k(\mathbf{x}) + \eta_k(t) \quad (31)$$

where $\eta_k(t)$ is a white noise that satisfies $\mathbb{E}[\eta_k(s)\eta_j(t)] = \sigma_{proc}^2 \delta_{kj} \delta(t-s)$ (where \mathbb{E} denotes the expectation). We define the flow $\varphi : \mathbb{R}^+ \times \mathbb{R}^n \times \Omega$, where Ω is the probability space, such that $t \mapsto \varphi(t, \mathbf{x}, \omega)$ is a solution to (31). In this case, the semigroup of Koopman operators is defined by (see e.g. [21])

$$U^t f(\mathbf{x}) = \mathbb{E}[f(\varphi(t, \mathbf{x}, \omega))]$$

and its infinitesimal generator is given by

$$Lf = \mathbf{F} \cdot \nabla f + \frac{\sigma_{proc}^2}{2} \Delta f$$

where $\Delta = \sum_k \partial^2 / \partial x_k^2$ denotes the Laplacian operator that accounts for diffusion. The infinitesimal generator is related to the so-called Kolmogorov backward equation.

Now we can show that the numerical scheme of the proposed identification method does not need to be adapted to take process noise into account. As explained in [36], the first step of the method (Section 3.1.1) is still valid for identifying the matrix $\bar{\mathbf{U}}$. In the second step (Section 3.1.2), the procedure is the same, except that one has to consider the Laplacian operator whose representation in the basis of monomials is

$$\bar{\mathbf{D}} = \sum_{j=1}^n \bar{\mathbf{D}}_j \in \mathbb{R}^{N \times N_0}$$

with

$$[\bar{\mathbf{D}}_j]_{il} = \begin{cases} \Psi_j(l)(\Psi_j(l) - 1) & \text{if } \Psi(i) = \Psi(l) - 2\mathbf{e}_j \\ 0 & \text{otherwise} \end{cases}$$

(where the index function Ψ is the one defined in Section 3.1.3). The equality (21) is then replaced by

$$\sum_{j=1}^n \sum_{k=1}^{N_F} \hat{w}_k^j \bar{\mathbf{L}}_k^j + \frac{\sigma^2}{2} \bar{\mathbf{D}} = [\bar{\mathbf{L}}_{\text{data}}]_{N_0}$$

where σ is an additional unknown. While the operators L_k^j map monomials of total degree m to monomials of total degree greater or equal to $m - 1$, the Laplacian operator maps monomials of total degree m to monomials of total degree $m - 2$. Therefore all nonzero entries of $\bar{\mathbf{D}}$ correspond to zero entries of $\bar{\mathbf{L}}_k^j$, so that the addition of the diffusion term only modifies entries of $\bar{\mathbf{L}}$ which do not depend on \hat{w}_k^j . In other words, the diffusion term does not affect the equalities on \hat{w}_k^j , whose solution is still given by (24). In Section 6.2, an example illustrates the robustness of the method against process noise.

4.3 Non polynomial vector fields

The method can be adapted to identify non-polynomial vector fields of the form (2), where the library functions h_k are not monomials. In this case, it is clear that the infinitesimal generator $L = F \cdot \nabla$, and in particular the operators $L_k^j = h_k \partial / \partial x_j$, might not map the monomials p_k onto polynomials. However, we can still perform the second step of the algorithm by considering the operators $P_N L_k^j |_{\mathcal{F}_N} : \mathcal{F}_N \rightarrow \mathcal{F}_N$, where \mathcal{F}_N is a subspace of polynomial functions. In this case, the projection $P_N : \mathcal{F} \rightarrow \mathcal{F}_N$ must be effectively computed, which was not necessary when the vector field was polynomial. This projection can be the usual orthogonal projection or the discrete L^2 projection minimizing the least squares error at the data points.

However, using the projection P_N adds an additional error to the finite-dimensional approximation of the operator. Instead, we prefer to consider a representation of the operators L_k^j from a subspace \mathcal{F}_{N_0} of polynomial functions of total degree less or equal to m_0 to an "augmented" subspace

$$\mathcal{F}'_N = \mathcal{F}_{N_0} \cup \text{span} \left(\left\{ L_k^j p_l \mid p_l \in \mathcal{F}_{N_0}, j = 1, \dots, n, k = 1, \dots, N_F \right\} \right)$$

that contains the image of the operators L_k^j . We can therefore compute the matrix representation of the operators $L_k^j |_{\mathcal{F}_{N_0}} : \mathcal{F}_{N_0} \rightarrow \mathcal{F}'_N$ without using the projection P'_N onto \mathcal{F}'_N , since $P'_N L_k^j |_{\mathcal{F}_{N_0}} = L_k^j |_{\mathcal{F}_{N_0}}$. In the case $\mathcal{F}_{N_0} = \text{span}(\{x_1, \dots, x_n\})$ (i.e. $m_0 = 1$),

we simply get the cartesian product of \mathcal{F}_{N_0} with the span of the library functions, i.e. $\mathcal{F}'_N = \mathcal{F}_{N_0} \times \text{span}(\{h_k, k = 1, \dots, N_F\})$.

We finally note that a more straightforward method is to perform a least squares regression on the values of the vector field at the sample points, values which can be obtained according to Remark 4. However, numerical experiments suggest that this method is less efficient than the above-mentioned method.

5 A dual lifting method for large systems

A major limitation of the main method presented in Section 3 (Algorithm 1) is that it might require a large number of data points. Indeed, the number of data points must be larger than the number of basis functions ($K \geq N$) to ensure that the discrete orthogonal projection (14) is well-defined. In the case of high-dimensional systems in particular, the number of basis functions is huge and is likely to exceed the number of available data points. Moreover, the algorithm might also be computationally intractable (e.g. computation of the matrix logarithm in (16)). In this section, we circumvent the above limitations by proposing a dual approach, which is developed in a K -dimensional “sample space” instead of the N -dimensional functional space. This method can be used when the number of basis functions is larger than the number of data points, i.e. $N \geq K$.

5.1 Description of the method

Similarly to the main lifting method, the dual method consists of three steps: lifting of the data, identification of the Koopman operator, and identification of the vector field. In the last step, the algorithm provides the value of the vector field at each data point, so that the dual method can be seen as an indirect method for time derivatives estimation. This is similar in essence to the vector field estimation detailed in Remark 4. The identification is achieved in a distributed way, a feature which makes the algorithm computationally efficient in the case of high-dimensional systems and well-suited to parallel computing.

5.1.1 First step: Lifting of the data

This step is similar to the first step of the main method (Section 3.1.1). But in this case, choosing the basis functions equal to the library functions of the vector field is not more convenient for the next steps. We will therefore consider monomials $g_k = p_k$, but also Gaussian radial basis functions

$$g_k(\mathbf{x}) = e^{-\gamma \|\mathbf{x} - \mathbf{x}_k\|^2}$$

with $k = 1, \dots, K$ and where $\gamma > 0$ is a parameter. We construct the data $K \times N$ matrices

$$\mathbf{P}_x = \begin{pmatrix} \mathbf{g}(\mathbf{x}_1)^T \\ \vdots \\ \mathbf{g}(\mathbf{x}_K)^T \end{pmatrix} \quad \mathbf{P}_y = \begin{pmatrix} \mathbf{g}(\mathbf{y}_1)^T \\ \vdots \\ \mathbf{g}(\mathbf{y}_K)^T \end{pmatrix} \quad (32)$$

where \mathbf{g} is the vector of basis functions g_k . When using Gaussian radial basis functions, the number of basis functions is equal to the number of samples (i.e. $N = K$) and therefore does not depend on the dimension n . This is particularly useful in the case of high-dimensional systems, where the matrices (32) should be of reasonable size. In Section 6, we will only use Gaussian radial basis functions.

5.1.2 Second step: Identification of the Koopman operator

In this section, we use a dual matrix representation of the Koopman operator, which is inspired (but slightly different) from a kernel-based approach developed in [37].

In the main method, we constructed the $N \times N$ matrix

$$\bar{\mathbf{U}}_N \approx \mathbf{P}_x^\dagger \mathbf{P}_y$$

which represents the operator $U_N^{T_s}$. Instead, we can consider the $K \times K$ matrix representation

$$\tilde{\mathbf{U}}_K \approx \mathbf{P}_y \mathbf{P}_x^\dagger = \mathbf{P}_x \bar{\mathbf{U}}_N \mathbf{P}_x^\dagger, \quad (33)$$

a construction which is similar to the original formulation of the Dynamic Mode Decomposition (DMD) algorithm³ [34]. The matrix \mathbf{P}_x can be interpreted as a change of coordinates, and $\tilde{\mathbf{U}}_K$ appears to be the matrix representation of U^{T_s} in the ‘‘sample space’’: for all $f \in \mathcal{F}_N$, we have

$$\begin{pmatrix} U^{T_s} f(\mathbf{x}_1) \\ \vdots \\ U^{T_s} f(\mathbf{x}_K) \end{pmatrix} \approx \tilde{\mathbf{U}}_K \begin{pmatrix} f(\mathbf{x}_1) \\ \vdots \\ f(\mathbf{x}_K) \end{pmatrix}.$$

We have seen that the j th column \mathbf{c}_j of $\bar{\mathbf{U}}_N$ satisfies $\mathbf{P}_x \mathbf{c}_j \approx (p_j(\mathbf{y}_1) \cdots p_j(\mathbf{y}_K))^T$ and corresponds to the projection (14) of $U^{T_s} p_j$ on \mathcal{F}_N (expressed in the basis of functions). Each of the K data points yields a constraint and there are N unknowns, so that $K \geq N$ is required. In contrast, the i th row \mathbf{r}_i of $\tilde{\mathbf{U}}_K$ can be seen, for all f , as the coefficients of the linear combination of the values $f(\mathbf{x}_1), \dots, f(\mathbf{x}_K)$ that is equal to $U^{T_s} f(\mathbf{x}_i)$. The row \mathbf{r}_i satisfies $r_i \mathbf{P}_x \approx (g_1(\mathbf{y}_i) \cdots g_N(\mathbf{y}_i))$, i.e. r_i is obtained by considering the N ‘‘test’’ functions g_j . In this case, each of the N functions yields a constraint and there are K unknowns, so that $K \leq N$ is required.

Remark 6. Following similar lines as in [37], we note that we have

$$\tilde{\mathbf{U}}_K \approx \mathbf{P}_y \mathbf{P}_x^\dagger = \mathbf{P}_y \mathbf{P}_x^T (\mathbf{P}_x \mathbf{P}_x^T)^\dagger \triangleq \mathbf{A} \mathbf{G}^\dagger$$

where the entries of \mathbf{A} and \mathbf{G} can be interpreted as the inner products

$$[\mathbf{A}]_{ij} = \mathbf{p}(\mathbf{x}_j)^T \mathbf{p}(\mathbf{y}_i), \quad [\mathbf{G}]_{ij} = \mathbf{p}(\mathbf{x}_j)^T \cdot \mathbf{p}(\mathbf{x}_i)$$

(Here, we consider without loss of generality that the matrices \mathbf{P}_x and \mathbf{P}_y are constructed with monomials.) The inner products can be approximated by a Gaussian kernel function $g(\mathbf{x}_i, \mathbf{x}_j) = g_j(\mathbf{x}_i)$, so that

$$[\mathbf{A}]_{ij} = [\mathbf{A}]_{ij} = g(\mathbf{x}_i, \mathbf{x}_j), \quad [\mathbf{G}]_{ij} = [\mathbf{A}]_{ij} = g(\mathbf{y}_i, \mathbf{x}_j).$$

In this context, constructing \mathbf{P}_x and \mathbf{P}_y with Gaussian radial basis functions is equivalent to constructing the inner-product matrices \mathbf{A} and \mathbf{G} . \diamond

Finally, similarly to (16), we compute the $K \times K$ matrix

$$\tilde{\mathbf{L}}_{\text{data}} = \frac{1}{T_s} \log(\mathbf{P}_y \mathbf{P}_x^\dagger). \quad (34)$$

³This would correspond exactly to DMD if the basis functions g_j were replaced by functions $g_j(x) = \varphi^{(j-1)t_s}(x)$.

5.1.3 Third step: Identification of the vector field

Using a similar idea as the one explained in Remark 4, we can directly identify the vector field at the different values \mathbf{x}_k and the coefficients w_k^j are then obtained by solving n separate regression problems.

Computation of the vector field $\mathbf{F}(\mathbf{x}_k)$. We assume that $\tilde{\mathbf{L}}_{\text{data}}$ is an approximation of the matrix representation of L in the sample space and we have

$$\begin{pmatrix} \mathbf{F}(\mathbf{x}_1) \cdot \nabla f(\mathbf{x}_1) \\ \vdots \\ \mathbf{F}(\mathbf{x}_K) \cdot \nabla f(\mathbf{x}_K) \end{pmatrix} = \begin{pmatrix} Lf(\mathbf{x}_1) \\ \vdots \\ Lf(\mathbf{x}_K) \end{pmatrix} \approx \tilde{\mathbf{L}}_{\text{data}} \begin{pmatrix} f(\mathbf{x}_1) \\ \vdots \\ f(\mathbf{x}_K) \end{pmatrix}.$$

Considering the above equality with the identity function $\mathbf{f}(\mathbf{x}) = \mathbf{x}$, we obtain an approximation $\hat{\mathbf{F}}$ of the vector field that is given by

$$\begin{pmatrix} \hat{\mathbf{F}}(\mathbf{x}_1)^T \\ \vdots \\ \hat{\mathbf{F}}(\mathbf{x}_K)^T \end{pmatrix} \approx \tilde{\mathbf{L}}_{\text{data}} \begin{pmatrix} \mathbf{x}_1^T \\ \vdots \\ \mathbf{x}_K^T \end{pmatrix}. \quad (35)$$

The choice of the functions f used to obtain (35) is arbitrary. However, considering monomials of degree one is natural and choosing more functions would yield an overconstrained problem which does not necessarily improve the accuracy of the result. Note also that an approach more similar to the main method is to compute (an approximation of) the matrix representation of $L = \mathbf{F} \cdot \nabla$ in the sampling space and compare it with $\tilde{\mathbf{L}}_{\text{data}}$. However, this does not yield better results.

Computation of the coefficients w_k^j . When the value of the vector field is known at every data points, we can find an estimation \hat{w}_k^j of the coefficients w_k^j by solving a regression problem. This problem is decoupled: for each $j = 1, \dots, n$, we have to solve

$$\hat{F}_j(\mathbf{x}_k) = \sum_{l=1}^{N_F} \hat{w}_j^l h_l(\mathbf{x}_k) \quad k = 1, \dots, K,$$

which takes the form

$$\begin{pmatrix} \hat{F}_j(\mathbf{x}_1) \\ \vdots \\ \hat{F}_j(\mathbf{x}_K) \end{pmatrix} = \mathbf{H}_{\mathbf{x}} \begin{pmatrix} \hat{w}_1^j \\ \vdots \\ \hat{w}_{N_F}^j \end{pmatrix} \quad (36)$$

with

$$\mathbf{H}_{\mathbf{x}} = \begin{pmatrix} \mathbf{h}(\mathbf{x}_1)^T \\ \vdots \\ \mathbf{h}(\mathbf{x}_K)^T \end{pmatrix} \quad (37)$$

and where \mathbf{h} is the vector of library functions h_k of the vector field. We do not make any assumption on these library functions, which are not necessarily monomials.

Since we can reasonably assume that most coefficients are zero, we can promote sparsity of the vector of coefficients \hat{w}_j^l by adding a penalty term, which yields the Lasso optimization problem [33]

$$\min_{\mathbf{w} \in \mathbb{R}^{N_F}} \left\| \mathbf{H}_{\mathbf{x}} \mathbf{w} - \begin{pmatrix} \hat{F}_j(\mathbf{x}_1) \\ \vdots \\ \hat{F}_j(\mathbf{x}_K) \end{pmatrix} \right\|_2^2 + \rho \|\mathbf{w}\|_1 \quad (38)$$

where ρ is a positive regularization parameter. Other techniques could also be used to infer \mathbf{w} from the values of the vector field (see e.g. [3, 25]). More generally, machine learning techniques could also be used to solve the regression problem (36).

5.2 Algorithm

The dual method is summarized in the following algorithm.

Algorithm 2 Dual lifting method for nonlinear system identification

Input: Snapshot pairs $\{(\mathbf{x}_k, \mathbf{y}_k)\}_{k=1}^K$, $\mathbf{x}_k \in \mathbb{R}^n$; basis functions $\{g_k\}_{k=1}^N$; library functions $\{h_k\}_{k=1}^{N_F}$.

Output: Estimates $\hat{\mathbf{F}}(\mathbf{x}_k)$ and \hat{w}_k^j .

- 1: **if** $N < K$ **then**
 - 2: Increase N (number of basis functions)
 - 3: **end if**
 - 4: Construct the $K \times N$ matrices $\mathbf{P}_{\mathbf{x}}$ and $\mathbf{P}_{\mathbf{y}}$ defined in (32)
 - 5: Compute the $K \times K$ matrix $\tilde{\mathbf{L}}_{\text{data}}$ defined in (34)
 - 6: Obtain $\hat{\mathbf{F}}(\mathbf{x}_k)$ with (35)
 - 7: Construct the $K \times N_F$ matrices $\mathbf{H}_{\mathbf{x}}$ defined in (37)
 - 8: For each j , solve the regression problem (36), e.g. solve the Lasso problem (38), to obtain \hat{w}_k^j
-

5.3 Theoretical results

We now show the convergence of Algorithm 2 in optimal conditions. Let $X \subset \mathbb{R}^n$ be a compact set that contains all the data points \mathbf{x}_k and assume that $\mathcal{F} = L^2(X)$ (where $\|\cdot\|$ is the L^2 norm). We consider a partition $\{X_k\}_{k=1}^K$ of X such that $\mathbf{x}_k \in X_k$ and $\mathbf{x}_j \notin X_k$ for all $j \neq k$ and such that the Lebesgue measure $\mu(X_k)$ of each set is equal, i.e. $\mu(X_k) = \mu(X)/K$. Let also $\tilde{\mathcal{F}}_K$ be the set of functions that are piecewise constant on this partition. Then, the matrix $\tilde{\mathbf{U}}_K$ can be interpreted as the matrix representation of the finite-rank operator $\tilde{U}_K : \tilde{\mathcal{F}}_K \rightarrow \tilde{\mathcal{F}}_K$ that minimizes

$$\sum_{l=1}^N \left\| \left(\tilde{P}_K U^{T_s} - \tilde{U}_K \tilde{P}_K \right) g_l \right\|^2 = \frac{\mu(X)}{K} \sum_{l=1}^N \left\| \begin{pmatrix} g_l(\mathbf{y}_1) \\ \vdots \\ g_l(\mathbf{y}_K) \end{pmatrix} - \tilde{\mathbf{U}}_K \begin{pmatrix} g_l(\mathbf{x}_1) \\ \vdots \\ g_l(\mathbf{x}_K) \end{pmatrix} \right\|^2, \quad (39)$$

where $\tilde{P}_K : \mathcal{F} \rightarrow \tilde{\mathcal{F}}_K$ is the projection operator such that $\tilde{P}_K f(\mathbf{x}) = f(\mathbf{x}_k)$ for all $\mathbf{x} \in X_k$.

We first prove the following lemma.

Lemma 2. Consider the semigroup of operators $U^t : L^2(X) \rightarrow L^2(X)$ and its infinitesimal generator $L : \mathcal{D}(L) \rightarrow L^2(X)$. Suppose that $\{g_l\}_{l=1}^\infty$, with $g_l \in C^1(X)$, form a complete basis of \mathcal{F} . If there exists $\tilde{L}_K : \tilde{\mathcal{F}}_K \rightarrow \tilde{\mathcal{F}}_K$ that satisfies

$$\left(\tilde{P}_K L - \tilde{L}_K \tilde{P}_K\right) g_l = 0 \quad (40)$$

for all $g_l \in \mathcal{F}$ with $l \leq K$ and so that it generates a strongly continuous semi-group $e^{\tilde{L}_K t}$, then

$$\left\| \left(\tilde{P}_K U^t - e^{\tilde{L}_K t} \tilde{P}_K\right) g_l \right\| \rightarrow 0$$

as $K \rightarrow \infty$.

Proof. Since the span of $\{g_l\}_{l=1}^\infty$ is dense in \mathcal{F} , for all $g \in C_1(X)$, there exists a sequence c_l such that $g \rightarrow \sum_l c_l g_l$ and we have

$$\left\| \left(\tilde{P}_K L - \tilde{L}_K \tilde{P}_K\right) g \right\| \leq \left\| \left(\tilde{P}_K L - \tilde{L}_K \tilde{P}_K\right) \left(g - \sum_{l=1}^\infty c_l g_l\right) \right\| + \left\| \sum_{l=1}^\infty c_l \left(\tilde{P}_K L - \tilde{L}_K \tilde{P}_K\right) g_l \right\| \rightarrow 0 \quad (41)$$

where we used (40) and the fact that $\tilde{P}_K L - \tilde{L}_K \tilde{P}_K$ is continuous on the subspace of continuously differentiable functions. Following similar lines as in the proof of [5, Theorem 3.5], we have

$$\begin{aligned} \left\| \left(\tilde{P}_K U^t - e^{\tilde{L}_K t} \tilde{P}_K\right) g_l \right\| &= \left\| \int_0^t \frac{d}{ds} \left(e^{\tilde{L}_K(t-s)} \tilde{P}_K U^s g_l \right) ds \right\| \\ &= \left\| \int_0^t e^{\tilde{L}_K(t-s)} \left(\tilde{L}_K \tilde{P}_K - \tilde{P}_K L \right) U^s g_l ds \right\| \rightarrow 0 \end{aligned}$$

where we used the chain rule (see e.g. [5, Lemma B.16]) and (41) with the continuous function $g = U^s g_l$. \square

Remark 7. The properties of $e^{\tilde{L}_K t}$ could be further investigated. In particular, the boundedness of $e^{\tilde{L}_K t}$ could possibly be obtained by considering Trotter-Kato approximation theorem to show that $\left\| \left(\tilde{P}_K U^t - e^{\tilde{L}_K \tilde{P}_K t}\right) f \right\| \rightarrow 0$, and then using the boundedness of $e^{\tilde{L}_K \tilde{P}_K t}$.

The following results show that Algorithm 2 provides exact estimates $\hat{\mathbf{F}}(\mathbf{x}_k)$ of the vector field in optimal conditions.

Theorem 2. Assume that the sample points $\mathbf{x}_k \in X$ are uniformly randomly distributed in a compact forward invariant set X , and consider $\mathbf{y}_k = \varphi^{T_s}(\mathbf{x}_k)$ (no measurement noise). Suppose that $\{g_l\}_{l=1}^\infty$, with $g_l \in C^1(X)$, form a complete, linearly independent basis of \mathcal{F} . If the Algorithm 2 is used with the data pairs $\{\mathbf{x}_k, \mathbf{y}_k\}_{k=1}^K$ and with basis functions g_l where $K = N$ (case 1) or such that $\sum_l \|\nabla g_l\|_{L^\infty(X)}^2 < \infty$ (case 2), then

$$\frac{1}{K} \sum_{k=1}^K \left\| \mathbf{F}(\mathbf{x}_k) - \hat{\mathbf{F}}(\mathbf{x}_k) \right\|^2 \rightarrow 0$$

as $K \rightarrow \infty$, $N \rightarrow \infty$, and $T_s \rightarrow 0$.

Proof. In the following, we denote by $\tilde{f}(\mathbf{x}_k)$ the vectors

$$\tilde{f}(\mathbf{x}_k) \triangleq \begin{pmatrix} f(\mathbf{x}_1) \\ \vdots \\ f(\mathbf{x}_K) \end{pmatrix}.$$

If $N = K$ (case 1), the minimization of (39) is not overconstrained and $\tilde{\mathbf{U}}_K$ satisfies

$$\tilde{g}_l(\mathbf{y}_k) - \tilde{\mathbf{U}}_K \tilde{g}_l(\mathbf{x}_k) = 0 \quad (42)$$

exactly for all l . In the other situation (case 2), we denote $\mathbf{x}'_k = \arg \min_{\mathbf{x}_k} |\mathbf{x}_k - \mathbf{y}_k|$ and it follows from (39) that

$$\begin{aligned} \sum_{l=1}^N \frac{1}{K} \left\| \tilde{g}_l(\mathbf{y}_k) - \tilde{\mathbf{U}}_K \tilde{g}_l(\mathbf{x}_k) \right\|^2 &= \min_{\mathbf{U}_K \in \mathbb{R}^{K \times K}} \sum_{l=1}^N \frac{1}{K} \left\| \tilde{g}_l(\mathbf{y}_k) - \mathbf{U}_K \tilde{g}_l(\mathbf{x}_k) \right\|^2 \\ &\leq \sum_{l=1}^N \frac{1}{K} \left\| \tilde{g}_l(\mathbf{y}_k) - \tilde{g}_l(\mathbf{x}'_k) \right\|^2 \\ &\leq \frac{1}{K} \sum_{k=1}^K \sum_{l=1}^N \|\nabla g_l\|_{L^\infty(X)}^2 \|\mathbf{x}'_k - \mathbf{y}_k\|^2 \rightarrow 0 \end{aligned}$$

since $\sum_{l=1}^N \|\nabla g_l\|_{L^\infty(X)}^2$ is bounded (case 2) and $\|\mathbf{x}'_k - \mathbf{y}_k\|$ is arbitrarily small as $K \rightarrow \infty$ (X is forward invariant). This implies that

$$\frac{1}{K} \left\| \tilde{g}_l(\mathbf{y}_k) - \tilde{\mathbf{U}}_K \tilde{g}_l(\mathbf{x}_k) \right\| \rightarrow 0 \quad (43)$$

as $K \rightarrow \infty$.

Moreover, since $\{g_l\}_{l=1}^N$ is a set of linearly independent functions, so is the set $\{\tilde{P}_K g_l\}_{l=1}^N$ in \mathcal{F}_K for K large enough. It follows that the operator \tilde{L}_K satisfying (40) exists. Then, Lemma 2 implies that

$$\frac{1}{K} \left\| \tilde{g}_l(\mathbf{y}_k) - e^{\tilde{\mathbf{L}}_K T_s} \tilde{g}_l(\mathbf{x}_k) \right\| \rightarrow 0$$

where $\tilde{\mathbf{L}}_K$ is the matrix representation of \tilde{L}_K . Combining with (42) or (43), we obtain

$$\frac{1}{K} \left\| \left(\tilde{\mathbf{U}}_K - e^{\tilde{\mathbf{L}}_K T_s} \right) \tilde{g}_l(\mathbf{x}_k) \right\| \leq \frac{1}{K} \left\| \tilde{\mathbf{U}}_K \tilde{g}_l(\mathbf{x}_k) - \tilde{g}_l(\mathbf{y}_k) \right\| + \frac{1}{K} \left\| \tilde{g}_l(\mathbf{y}_k) - e^{\tilde{\mathbf{L}}_K T_s} \tilde{g}_l(\mathbf{x}_k) \right\| \rightarrow 0.$$

Since the vectors $\tilde{g}_l(\mathbf{x}_k)$ form a linearly independent basis in \mathbb{R}^K as $K \rightarrow \infty$, we have $\tilde{\mathbf{U}}_K - e^{\tilde{\mathbf{L}}_K T_s} \rightarrow 0$ or equivalently $\frac{1}{T_s} \log \tilde{\mathbf{U}}_K - \frac{1}{T_s} \log e^{\tilde{\mathbf{L}}_K T_s} \rightarrow 0$. Since there is no measurement noise, (33) and (34) imply that $\tilde{\mathbf{L}}_{\text{data}} = \frac{1}{T_s} \log \tilde{\mathbf{U}}_K$ and, in addition, $\frac{1}{T_s} \log e^{\tilde{\mathbf{L}}_K T_s} = \tilde{\mathbf{L}}_K$ as $T_s \rightarrow 0$. Hence, we obtain $\tilde{\mathbf{L}}_{\text{data}} = \tilde{\mathbf{L}}_K$. Denoting by $x^{(j)}$ the j th component of \mathbf{x} , we have

$$\frac{1}{K} \sum_{k=1}^K \left(F_j(\mathbf{x}_k) - \hat{F}_j(\mathbf{x}_k) \right)^2 = \frac{1}{K} \left\| \begin{pmatrix} F_j(\mathbf{x}_1) \\ \vdots \\ F_j(\mathbf{x}_K) \end{pmatrix} - \tilde{\mathbf{L}}_{\text{data}} \begin{pmatrix} x_1^{(j)} \\ \vdots \\ x_K^{(j)} \end{pmatrix} \right\|^2 = \frac{1}{K} \left\| \begin{pmatrix} F_j(\mathbf{x}_1) \\ \vdots \\ F_j(\mathbf{x}_K) \end{pmatrix} - \tilde{\mathbf{L}}_K \begin{pmatrix} x_1^{(j)} \\ \vdots \\ x_K^{(j)} \end{pmatrix} \right\|^2$$

or equivalently

$$\frac{\mu(X)}{K} \sum_{k=1}^K \left(F_j(\mathbf{x}_k) - \hat{F}_j(\mathbf{x}_k) \right)^2 = \left\| \tilde{P}_K L x^{(j)} - \tilde{L}_K \tilde{P}_K x^{(j)} \right\|^2$$

where $\mu(X)$ denotes the Lebesgue measure of X . Finally, since the span of $\{g_l\}_{l=1}^\infty$ is dense in \mathcal{F} , there exists a sequence c_l such that $x^{(j)} \rightarrow \sum_l c_l g_l$ and we have

$$\left\| \left(\tilde{P}_K L - \tilde{L}_K \tilde{P}_K \right) x^{(j)} \right\| \leq \left\| \left(\tilde{P}_K L - \tilde{L}_K \tilde{P}_K \right) \left(x^{(j)} - \sum_{l=1}^\infty c_l g_l \right) \right\| + \left\| \sum_{l=1}^\infty c_l \left(\tilde{P}_K L - \tilde{L}_K \tilde{P}_K \right) g_l \right\| \rightarrow 0$$

where we used (40) and the fact that $\tilde{P}_K L - \tilde{L}_K \tilde{P}_K$ is continuous on the subspace of continuously differentiable functions. This concludes the proof. \square

Theorem 2 proves the convergence of Algorithm 2 when it is used with Gaussian radial basis functions and monomials (with $X \subset [-1, 1]^n$). Indeed, these bases are dense in $L^2(X)$ (see [26] for Gaussian radial basis functions) and linearly independent. Moreover, they satisfy the additional technical assumptions of the theorem.

6 Illustrative examples

The goal of this section is to provide several examples to illustrate the two methods, including some extensions of the main method. We do not provide here an extensive study of the performance with respect to the choice of basis functions and parameters, considering that this is out of the scope of the present paper.

We consider simulated data and, unless otherwise stated, we add a Gaussian measurement noise with zero mean and standard deviation $\sigma_{meas} = 0.01$ (see (4)).

6.1 Main method

We use the lifting method described in Section 3, with the parameters $m_0 = 1$ and $m_F = 3$ ($m_1 = m_0 + m_F - 1 = 3$). We consider three systems that exhibit different types of behaviors.

1. Van der Pol oscillator: the dynamics are given by

$$\begin{aligned} \dot{x}_1 &= x_2 \\ \dot{x}_2 &= (1 - x_1^2)x_2 - x_2 \end{aligned}$$

and possess a stable limit cycle.

2. Unstable equilibrium: the dynamics are given by

$$\begin{aligned} \dot{x}_1 &= 3x_1 + 0.5x_2 - x_1x_2 + x_2^2 + 2x_1^3 \\ \dot{x}_2 &= 0.5x_1 + 4x_2 \end{aligned}$$

and are characterized by an unstable equilibrium at the origin.

3. Chaotic Lorenz system: the dynamics are given by

$$\begin{aligned}\dot{x}_1 &= 10(x_2 - x_1) \\ \dot{x}_2 &= x_1(28 - x_3) - x_2 \\ \dot{x}_3 &= x_1x_2 - 8/3x_3\end{aligned}$$

and exhibit a chaotic behavior.

A set of K data pairs is generated by taking snapshots at times $\{0, T_s, \dots, K/rT_s\}$ from r trajectories of these systems. For the first two systems, we consider a setting that is not well-suited to a direct estimation of the derivatives: the sampling period T_s is (reasonably) large and only two or three data points are taken on each trajectory. The identification of the third system, however, requires a smaller sampling period and a larger number of samples. Parameters used to generate the datasets are summarized in the left part of Table 1.

For each model, Algorithm 1 yields the estimates \hat{w}_k^j of the coefficients w_k^j . We compute the root mean square error

$$\text{RMSE} = \sqrt{\frac{1}{nN_F} \sum_{j=1}^n \sum_{k=1}^{N_F} \left((w_k^j) - (\hat{w}_k^j) \right)^2} \quad (44)$$

and the normalized root mean square error $\text{NRMSE} = \text{RMSE}/\bar{w}$, where \bar{w} is the average value of the nonzero coefficients $|w_k^j|$. The RMSE and NRMSE values averaged over 50 experiments are small (Table 1) and show that the lifting method achieves good performance to identify each system with a fairly low number of samples.

	Sampling period (T_s)	Total number of data pairs (K)	Number of trajectories (r)	Initial conditions	RMSE	NRMSE
1. Van der Pol	0.5	30	15	$[-1, 1]^2$	0.023	0.023
2. Unstable	0.2	20	20	$[-0.5, 0.5]^2$	0.150	0.087
3. Lorenz	0.033	300	20	$[-20, 20]^3$	0.451	0.059

Table 1: Features of the datasets and (normalized) root mean square error averaged over 50 simulations.

For the three systems described above, we also consider the effect of the sampling period T_s on the performance of the method (Figure 2). In the noiseless case, the NRMSE decreases (exponentially) as the sampling period decreases. This is in agreement with the fact that the NRMSE tends to zero as $T_s \rightarrow 0$ (Theorem 1). With measurement noise, this is not the case since the method is biased. In this case, small values of the sampling period make the method more sensitive to noise, so that the minimal (nonzero) value of the NRMSE is obtained with an intermediate value of the sampling period.

Next, the approximation of the vector field obtained with (25) is compared with the approximation obtained directly from data through (central) finite differences, i.e.

$$\hat{\mathbf{F}}(\mathbf{x}_k) = \frac{\mathbf{x}_{k+1} - \mathbf{x}_{k-1}}{2T_s}.$$

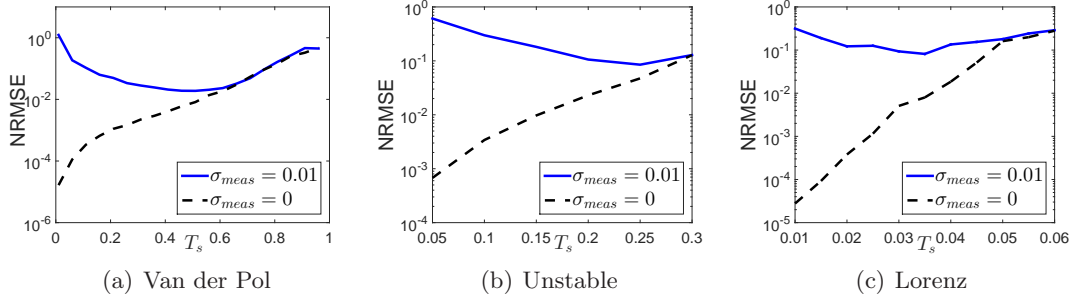


Figure 2: Effect of the sampling period on the normalized root mean square error (averaged over 50 experiments). Parameters are given in Table 1.

We consider the three systems and compute the normalized root mean square error on the vector field

$$NRMSE_F = \sqrt{\frac{\sum_{j=1}^n \sum_{k=2}^K \|\hat{\mathbf{F}}(\mathbf{x}_k) - \mathbf{F}(\mathbf{x}_k)\|^2}{(K-1)}} / \frac{1}{K-1} \sum_{k=2}^K \|\mathbf{F}(\mathbf{x}_k)\|$$

averaged over 10 experiments⁴, for different values of the sampling period. The results are shown in Figure 3. For each system, we observe that the approximation obtained with the lifting method provides an estimate with an acceptable error (e.g. $NRMSE_F < 0.1$) for larger values of the sampling period than the direct finite difference method. This approximation is also characterized by a clear transition at a critical value of the sampling period, above which the NRMSE sharply increases (not observed with the unstable system, for which the critical value is beyond the maximal integration time). These results demonstrate the need of considering an indirect method to estimate the vector field (and therefore identify the system) when the sampling period is large.

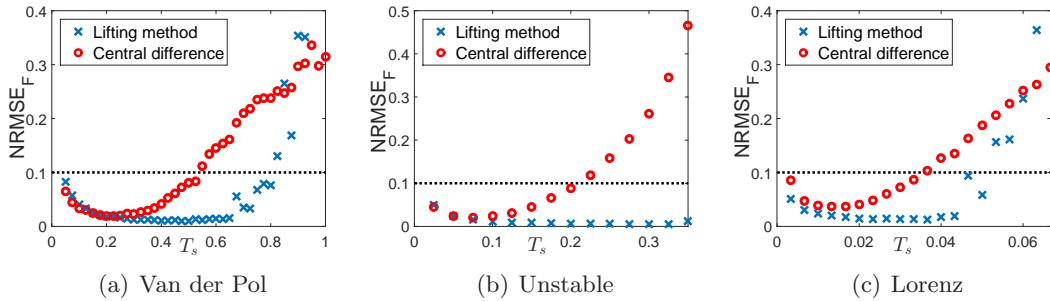


Figure 3: Comparison of the normalized root mean square error on the vector field estimated with the lifting method and with a finite difference method (averaged over 10 experiments). The parameters are the same as in Table 1, except for the unstable system where $K = 40$ (2 data pairs on each trajectory) and the initial conditions are in the set $[-0.1, 0.1]^2$.

⁴We discarded experiments where the matrix K has nonpositive eigenvalues, i.e. when the logarithm of K is not a real matrix.

6.2 Extensions

We now illustrate several extensions of the lifting method mentioned in Section 4: systems with inputs, process noise, non-polynomial vector fields.

Input and process noise. We consider the forced Duffing system

$$\dot{x}_1 = x_2 \tag{45}$$

$$\dot{x}_2 = x_1 - x_1^3 - 0.2x_2 + 0.2x_1^2 \cos(t) \tag{46}$$

and generate $K = 250$ snapshot data pairs from 5 trajectories (50 on each), with initial conditions on $[-1, 1]^2$. The lifting method provides a good estimation of the vector field (including the forcing term $0.2x_1^2 \cos(t)$). The RMSE (see Equation 44) and NRMSE computed over all coefficients (including those related to the forcing term) are given in Table 2 for different values of the sampling period. Note that we use again the parameters $m_0 = 1$ and $m_F = 3$.

Sampling period (T_s)	RMSE	NRMSE
0.2	0.032	0.046
0.4	0.031	0.045
0.6	0.057	0.084

Table 2: (Normalized) root mean square error (averaged over 50 experiments) related to the identification of the forced Duffing system.

Now, we replace the forcing term in (46) by the white noise $\eta(t)$ with different values of the standard deviation σ_{proc} (note that we still add measurement noise with $\sigma_{meas} = 0.01$). We generate $K = 500$ snapshot data pairs from 10 trajectories computed with the Euler-Maruyama scheme, with initial conditions on $[-1, 1]^2$. The sampling period is equal to $T_s = 0.2$. As shown in Table 3, the error is small even with strong process noise, suggesting that the method is robust against process noise.

Noise strength (σ_{proc})	RMSE	NRMSE
0.2	0.063	0.079
0.4	0.065	0.082
0.6	0.074	0.092
0.8	0.067	0.084
0.1	0.094	0.117

Table 3: (Normalized) root mean square error (averaged over 10 experiments) related to the identification of the Duffing system with process noise.

Non polynomial vector fields. In this example, we consider a genetic toggle switch (see e.g. [6])

$$\begin{aligned}\dot{x}_1 &= -x_1 + 2x_2 \\ \dot{x}_2 &= -x_2 + \frac{2}{1+x_3^2} \\ \dot{x}_3 &= -2x_3 + 2x_4 \\ \dot{x}_4 &= -2x_4 + \frac{1}{1+x_1^3}\end{aligned}$$

and we generate $K = 50$ snapshot data pairs from 50 trajectories, with initial conditions on $[0, 1]^4$. The sampling period is $T_s = 0.1$. Since the vector field is not polynomial, we use the extension presented in Section 4.3. The basis functions are the 5 monomials of total degree 0 and 1 (i.e. $m_0 = 1$ and $m_F = 1$), to which we add 12 Hill functions

$$\frac{1}{1+x_k^l} \quad k = \{1, 2, 3, 4\}, \quad l = \{1, 2, 3\}. \quad (47)$$

When there is no measurement noise, all coefficients (including those related to non-polynomial terms) are inferred correctly and we obtain a NRMSE equal to 0.008 (averaged over 50 experiments). However, the results are sensitive to noise in this case. With a measurement noise with $\sigma_{meas} = 0.001$, the NRMSE increases to 0.494. As shown in Section 6.3, the dual method is more robust to noise in this case.

6.3 Dual method

We illustrate the dual method in the case of a non-polynomial vector field. The main interest of the method, however, is its use with high-dimensional datasets, where the number of basis functions N is (much) larger than the number of sample points K . This will be illustrated in the next section.

The dual method requires to solve a regression problem. When $K < N_F$, we solve the (underconstrained) Lasso problem (38) with the MATLAB toolbox “yall1” [38, 40] (L1-L2 problem, with the parameter $\rho = 0.01$). When $K \geq N_F$, we solve the (overconstrained) problem (38) with the MATLAB function “lasso” (with the parameter $\lambda = 1/K$). Note that the value of the regularization parameter might not be optimal in all cases, but we did not extensively study its effect on the performance of the algorithm. In the following, we only use Gaussian radial basis functions with $\gamma = 0.1$ or $\gamma = 0.01$. Numerical simulations performed with monomial bases (not shown here) yield similar results for small dimensions, but are less accurate and more computationally expensive for large dimensions.

We consider the toggle switch system introduced in Section 6.2. Sample points are generated in the same conditions (i.e. $K = 50$, $T_s = 0.1$). We consider Gaussian radial basis functions with $\gamma = 0.1$ and 17 library functions (5 monomials of total degree 0 and 1, and 12 Hill functions (47)). With no noise, the NRMSE (averaged over 50 experiments) is equal to 0.064, which is worse than with the main method (Section 6.2). However, we obtain a NRMSE equal 0.117 with $\sigma_{meas} = 0.001$ and equal to 0.637 with $\sigma_{meas} = 0.01$. This shows that, in this case, the dual method is more robust to measurement noise than the main method.

6.4 Application to network identification

In the context of dynamical systems, each state can be seen as the node of a network. Moreover, a link can be drawn from node i to node j if the dynamics of the state x_j depends on the state x_i . Under the assumption that the vector field is of the form (2), there is a link from node i to node j if there is at least one nonzero coefficient w_k^j such that the corresponding library function h_k depends on x_i .

Network reconstruction aims at predicting links between states from data, a goal which is equivalent to finding nonzero coefficients w_k^j in our setting. We will consider that estimated coefficients \hat{w}_k^j with a small absolute value are mainly due to measurement noise and have an exact value w_k^j equal to zero. Hence, we decide that a link is present in the network only if the related value $|\hat{w}_k^j|$ is above a given threshold. To evaluate the performance of the method, one can compute the true positive rate (i.e. number of correctly identified links divided by the actual number of links) and the false positive rate (i.e. number of incorrectly identified links divided by the actual number of missing links). Varying the threshold value, we can plot the true positive rate against the false positive rate, which corresponds to the receiver operating characteristic (ROC) curve. If the area under the ROC curve (AUROC) is close to one, the network inference method provides good results (bad result correspond to a value close to 0.5).

Kuramoto oscillators. We consider a network of n Kuramoto phase oscillators

$$\dot{\theta}_i = \omega_i + \frac{C}{n} \sum_{j=1}^n a_{ij} \sin(\theta_j - \theta_i) \quad i = 1, \dots, n$$

with $\theta_i \in [0, 2\pi)$. The coupling strength is set to $C = 10$ and the natural frequencies ω_i are uniformly randomly distributed on $[0, 0.1]$. The values a_{ij} are the entries of the weighted adjacency matrix of a random Erdős-Rényi graph (with a probability $p_{link} = 0.3$ for any two nodes to be connected). The link weights are uniformly randomly distributed on $[0, 1]$.

For two networks ($n = 20$ and $n = 100$), we generate K sample pairs from $K/5$ trajectories (5 data pairs on each trajectory), with $T_s = 0.2$. Initial conditions are uniformly distributed on $[0, 2\pi)^n$. Note that we do not consider data points on $[0, 2\pi)$ but on the real line \mathbb{R} (i.e. without the modulo operation) where there is no discontinuity between 0 and 2π . We use the dual method with Gaussian radial basis functions (with $\gamma = 0.1$) and with $N_F = n$ library functions

$$\{1, \sin(\theta_1 - \theta_i), \dots, \sin(\theta_{i-1} - \theta_i), \sin(\theta_{i+1} - \theta_i), \dots, \sin(\theta_n - \theta_i)\}$$

for the i th component of the vector field. ROC curves are shown in Figure 4 and the results are summarized in Table 4, for different values of K and σ_{meas} . They show that the dual method achieves good performance to reconstruct the whole network. In particular, with high threshold values, one can infer many true positive links with no false positive link.

Network with nonlinear couplings. We consider a network where each state is directly influenced by other states through n_{inter} quadratic and cubic nonlinearities. Each nonlinear interaction depends on at most two states. The dynamics of the system are given by

$$\dot{x}_j = -\xi_j x_j + \sum_{k=1}^{n_{inter}} \zeta_{j,k} x_{\nu_1(j,k)}^{\sigma_1(j,k)} x_{\nu_2(j,k)}^{\sigma_2(j,k)} \quad j = 1, \dots, n \quad (48)$$

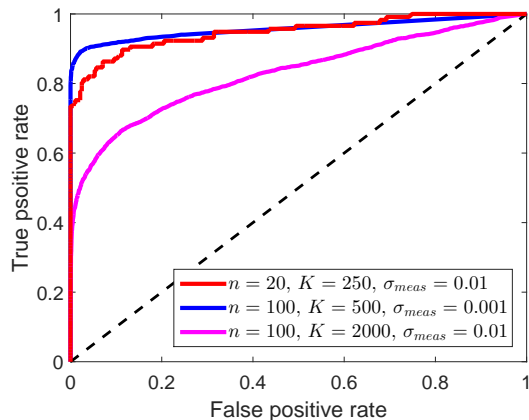


Figure 4: ROC curves obtained with the dual method for the reconstruction of a network of Kuramoto oscillators.

n	K	σ_{meas}	AUROC
20	250	0.01	0.95
100	500	0.001	0.96
100	2000	0.01	0.83

Table 4: Results obtained with the dual method for the reconstruction of a network of Kuramoto oscillators.

where the coefficients ξ_j are chosen according to a uniform distribution on $[0, 1]$ and $\zeta_{j,k}$ are distributed according to a Gaussian distribution of zero mean and standard deviation equal to one. The map $\nu = (\nu_1, \nu_2) : \{1, \dots, n\} \times \{1, \dots, n_{inter}\} \rightarrow \{1, \dots, n\}^2$ randomly selects the subscripts and the map $\sigma = (\sigma_1, \sigma_2) : \{1, \dots, n\} \times \{1, \dots, n_{inter}\}^2 \rightarrow \{0, 1, 2, 3\}$ randomly selects the exponents in such a way that $\sigma_1(j, k) + \sigma_2(j, k) \in \{2, 3\}$. The first term in (48) is a linear term that ensures local stability of the origin. For several network sizes ($n \in \{20, 50, 100\}$), we generate K samples from $K/2$ trajectories (2 data pairs on each trajectory), with $T_s = 0.5$. Initial conditions are uniformly randomly distributed on $[-0.5, 0.5]^n$.

Although we could also consider the main method for small networks (typically $n \leq 20$), we use only the dual method with Gaussian radial basis functions (with $\gamma = 0.01$). The library functions are monomials of total degree less or equal to 3. The method provides an accurate estimation of the vector field and a good reconstruction of the network (Table 5). The ROC curves depicted in Figure 5(a) show that most of half of the links can be inferred with no false positive link (with high threshold values). As shown in Figure 5(b-d), the method is also efficient to infer the nature of the interactions (e.g. quadratic, cubic). Taking advantage of sparsity, it uses not more than 1000 sample points to identify up to $17 \cdot 10^6$ coefficients (most of which are zero). We finally note that, for larger networks, the use of monomials as library functions becomes too demanding in terms of memory. In this case, the dual method can still be used to estimate the value of the vector field at the sample points, but should be combined with other (regression) methods to infer the network.

n	n_{inter}	K	AUROC	NRMSE
20	5	200	0.94	0.019
50	15	600	0.87	0.015
100	10	1000	0.91	0.004

Table 5: Results obtained with the dual method for the reconstruction of a network with quadratic and cubic interactions.

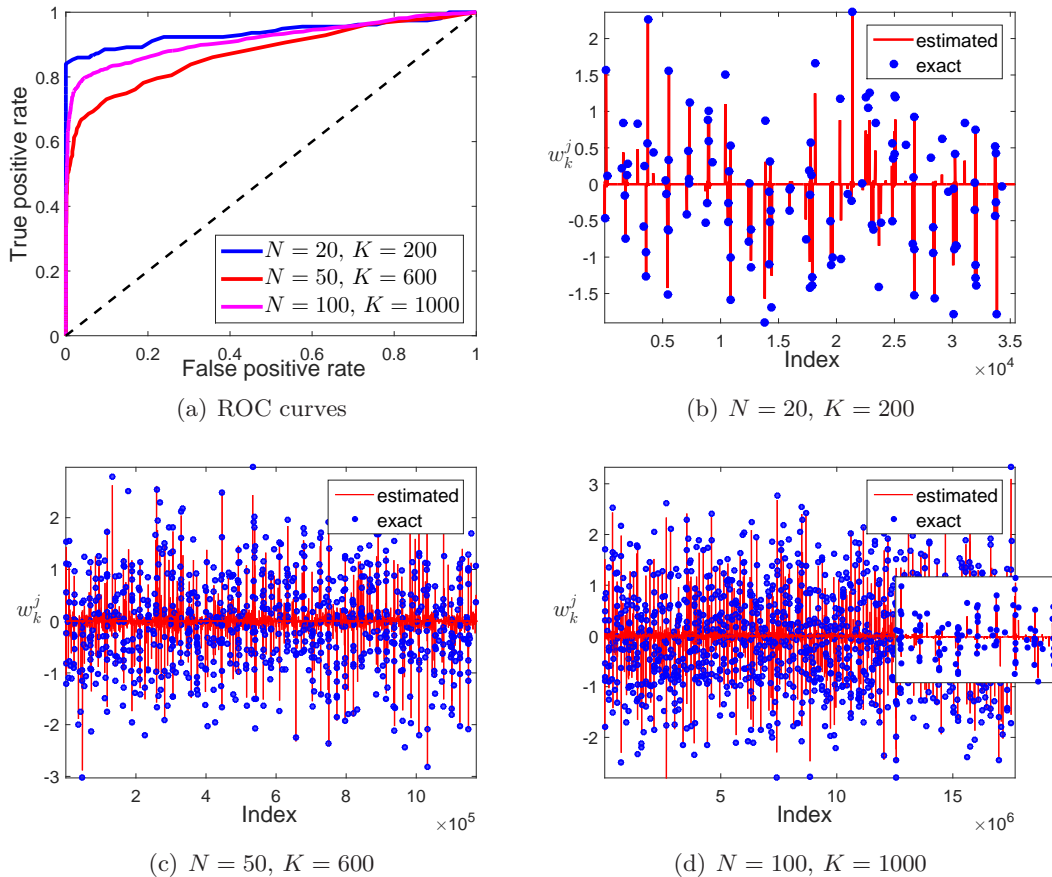


Figure 5: ROC curves and vector field coefficients obtained with the dual method for the reconstruction of a network with quadratic and cubic interactions. In (d), the inset shows a close-up of some estimated coefficients.

7 Conclusion

We have proposed a novel method for nonlinear systems identification. This method relies on a lifting technique developed in an operator-theoretic framework: it aims at identifying the linear Koopman operator in the space of observables. Key advantages of the method are that numerical schemes rely only on linear techniques and do not require the estimation of state time derivatives. For these reasons, this is a promising alternative to direct identification methods. As shown with several examples, the method is efficient to recover the vector field of several classes of systems, even from small time series with low sampling rate. Moreover, a

dual method is also proposed to identify high-dimensional systems and is successfully applied to network reconstruction.

The results presented in this paper open the door to further developments and improvements of lifting techniques for nonlinear systems identification, some of which are related to recent advances in Koopman operator theory. For instance, identification lifting techniques with dictionary learning could be developed [16]. Extensions to general vector fields might also be considered, possibly without using library functions. Toward this end, lifting techniques could be combined with other methods: identify unknown parameters with Kalman filtering [24], consider rational functions in the vector field with alternating directions method [17], apply machine learning regression techniques on time derivatives estimated with the dual method, etc. Moreover, we might improve the method robustness to (measurement) noise and provide numerical schemes that are unbiased and consistent. In this context, Bayesian inference could be considered as a relevant approach. A careful study of the matrix logarithm used in the lifting method could also help to select the good branch (instead of the principal one), a strategy which might improve the performances when the sampling rate is low. Finally, theoretical results could also be obtained to provide bounds on the estimation error.

Acknowledgments

The authors acknowledge J. Winkin and F. Lamoline for fruitful discussion and suggestions, and for their help in the proofs presented in the manuscript. They also wish to thank S. Brunton and N. Kutz for suggesting Kuramoto oscillators in the reconstruction problem. The authors acknowledge support from the Luxembourg National Research Fund. This paper presents research results of the Belgian Network DYSCO (Dynamical Systems, Control, and Optimization), funded by the Interuniversity Attraction Poles Programme initiated by the Belgian Science Policy Office. This research used resources of the "Plateforme Technologique de Calcul Intensif (PTCI)" located at the University of Namur, Belgium, which is supported by the F.R.S.-FNRS under the convention No. 2.5020.11. The PTCI is member of the "Consortium des Équipements de Calcul Intensif (CÉCI)".

References

- [1] H. ARBABI AND I. MEZIĆ, *Ergodic theory, Dynamic Mode Decomposition and computation of spectral properties of the Koopman operator*, arXiv preprint arXiv:1611.06664, (2016).
- [2] S. L. BRUNTON, J. L. PROCTOR, AND J. N. KUTZ, *Sparse identification of nonlinear dynamics with control (SINDYc)*, in Proceedings of the IFAC Conference, vol. 49, 2016, pp. 710–715. arXiv preprint arXiv:1605.06682.
- [3] S. L. BRUNTON, L. P. PROCTOR, AND J. N. KUTZ, *Discovering governing equations from data by sparse identification of nonlinear dynamical systems*, Proceedings of the National Academy of Sciences, 113 (2016), pp. 3932–3937.
- [4] M. BUDIŠIĆ, R. MOHR, AND I. MEZIĆ, *Applied Koopmanism*, Chaos, 22 (2012), pp. 047510–047510.

- [5] K.-J. ENGEL AND R. NAGEL, *One-parameter semigroups for linear evolution equations*, vol. 194, Springer Science & Business Media, 1999.
- [6] T. GARDNER, C. R. CANTOR, AND J. J. COLLINS, *Construction of a genetic toggle switch in escherichia coli*, *Nature*, 403 (2000), pp. 339–342.
- [7] R. HABER AND H. UNBEHAUEN, *Structure identification of nonlinear dynamic systems—a survey on input/output approaches*, *Automatica*, 26 (1990), pp. 651–677.
- [8] E. KAISER, J. N. KUTZ, AND S. L. BRUNTON, *Data-driven discovery of koopman eigenfunctions for control*. arXiv preprint arXiv:1707.01146, 2017.
- [9] N. KAZANTZIS AND C. KRAVARIS, *Time-discretization of nonlinear control systems via Taylor methods*, *Computers & chemical engineering*, 23 (1999), pp. 763–784.
- [10] B. O. KOOPMAN, *Hamiltonian systems and transformation in Hilbert space*, *Proceedings of the National Academy of Sciences of the United States of America*, 17 (1931), p. 315.
- [11] M. KORDA AND I. MEZIĆ, *Linear predictors for nonlinear dynamical systems: Koopman operator meets model predictive control*, arXiv preprint arXiv:1611.03537, (2016).
- [12] ———, *On convergence of extended dynamic mode decomposition to the Koopman operator*, arXiv preprint arXiv:1703.04680, (2017).
- [13] Y. LAN AND I. MEZIĆ, *Linearization in the large of nonlinear systems and Koopman operator spectrum*, *Physica D*, 242 (2013), pp. 42–53.
- [14] A. LASOTA AND M. C. MACKEY, *Chaos, Fractals, and Noise: stochastic aspects of dynamics*, Springer-Verlag, 1994.
- [15] I. LEONTARITIS AND S. A. BILLINGS, *Input-output parametric models for non-linear systems part i: deterministic non-linear systems*, *International journal of control*, 41 (1985), pp. 303–328.
- [16] Q. LI, F. DIETRICH, E. M. BOLLT, AND I. G. KEVREKIDIS, *Extended dynamic mode decomposition with dictionary learning: a data-driven adaptive spectral decomposition of the Koopman operator*. arXiv preprint arXiv:1707.00225, 2017.
- [17] N. M. MANGAN, S. L. BRUNTON, J. L. PROCTOR, AND J. N. KUTZ, *Inferring biological networks by sparse identification of nonlinear dynamics*, *IEEE Transactions on Molecular, Biological and Multi-Scale Communications*, 2 (2016), pp. 52–63.
- [18] A. MAUROY AND J. GONCALVES, *Linear identification of nonlinear systems: A lifting technique based on the Koopman operator*, in *Proceedings of the 55th IEEE Conference on Decision and Control*, 2016, pp. 6500–6505.
- [19] A. MAUROY AND I. MEZIĆ, *Global stability analysis using the eigenfunctions of the Koopman operator*, *IEEE Transactions On Automatic Control*, 61 (2016), pp. 3356–3369.

- [20] A. MAUROY AND A. SOOTLA, *Geometric properties of isostables and basins of attraction of monotone systems*. to appear in IEEE Transactions on Automatic Control, 2017.
- [21] I. MEZIĆ, *Spectral properties of dynamical systems, model reduction and decompositions*, Nonlinear Dynamics, 41 (2005), pp. 309–325.
- [22] D. MÜLLER, A. OTTO, AND G. RADONS, *From dynamical systems with time-varying delay via circle maps to koopmanism*. arXiv preprint arXiv:1701.05136, 2017.
- [23] K. S. NARENDRA AND K. PARTHASARATHY, *Identification and control of dynamical systems using neural networks*, IEEE Transactions on neural networks, 1 (1990), pp. 4–27.
- [24] W. PAN, F. MENOLASCINA, AND G.-B. STAN, *Online model selection for synthetic gene networks*, in Proceedings of the 55th IEEE Conference on Decision and Control, IEEE, 2016, pp. 776–782.
- [25] W. PAN, Y. YUAN, J. GONCALVES, AND G.-B. STAN, *A sparse Bayesian approach to the identification of nonlinear state-space systems*, IEEE Transactions On Automatic Control, 61 (2016), pp. 182–187.
- [26] J. PARK AND I. W. SANDBERG, *Universal approximation using radial-basis-function networks*, Neural computation, 3 (1991), pp. 246–257.
- [27] L. P. PROCTOR, S. L. BRUNTON, AND J. N. KUTZ, *Generalizing Koopman operator theory to allow for inputs and control*. <http://arxiv.org/abs/1602.07647>.
- [28] C. W. ROWLEY, I. MEZIĆ, S. BAGHERI, P. SCHLATTER, AND D. S. HENNINGSON, *Spectral analysis of nonlinear flows*, Journal of Fluid Mechanics, 641 (2009), pp. 115–127.
- [29] P. J. SCHMID, *Dynamic mode decomposition of numerical and experimental data*, Journal of Fluid Mechanics, 656 (2010), pp. 5–28.
- [30] J. SJÖBERG, Q. ZHANG, L. LJUNG, A. BENVENISTE, B. DELYON, P.-Y. GLORENEC, H. HJALMARSSON, AND A. JUDITSKY, *Nonlinear black-box modeling in system identification: a unified overview*, Automatica, 31 (1995), pp. 1691–1724.
- [31] A. SURANA AND A. BANASZUK, *Linear observer synthesis for nonlinear systems using Koopman operator framework*, in Proceedings of the IFAC conference, vol. 49, Elsevier, 2016, pp. 716–723.
- [32] Y. SUSUKI AND I. MEZIĆ, *Nonlinear Koopman modes and power system stability assessment without models*, IEEE Transactions On Power Systems, 29 (2014), pp. 899–907.
- [33] R. TIBSHIRANI, *Regression shrinkage and selection via the lasso*, Journal of the Royal Statistical Society. Series B (Methodological), (1996), pp. 267–288.
- [34] J. H. TU, C. W. ROWLEY, D. M. LUCHTENBURG, S. L. BRUNTON, AND J. N. KUTZ, *On dynamic mode decomposition: Theory and applications*, Journal of Computational Dynamics, 1 (2014), pp. 391 – 421.

- [35] N. WIENER, *Nonlinear problems in random theory*, Nonlinear Problems in Random Theory, by Norbert Wiener, pp. 142. ISBN 0-262-73012-X. Cambridge, Massachusetts, USA: The MIT Press, August 1966.(Paper), (1966), p. 142.
- [36] M. O. WILLIAMS, I. G. KEVREKIDIS, AND C. W. ROWLEY, *A data-driven approximation of the Koopman operator: Extending dynamic mode decomposition*, Journal of Nonlinear Science, (2015), pp. 1–40.
- [37] M. O. WILLIAMS, C. W. ROWLEY, AND I. G. KEVREKIDIS, *A kernel-based approach to data-driven Koopman spectral analysis*, Journal of Computational Dynamics, 2 (2015), pp. 247–265.
- [38] J. YANG AND Y. ZHANG, *Alternating direction algorithms for l1-problems in compressive sensing*, SIAM Journal on Scientific Computing, 33 (2011), pp. 250–278.
- [39] Z. YUE, J. THUNBERG, L. LJUNG, AND J. GONCALVES, *Identification of Sparse Continuous-Time Linear Systems with Low Sampling Rate: Exploring Matrix Logarithms*. <https://arxiv.org/abs/1605.08590>.
- [40] Y. ZHANG, J. YANG, AND Y. W., *YALL1: Your ALgorithms for L1*, yall1.blogs.rice.edu, 2011.